Analysis of the spatially-resolved metabolic distribution for unraveling the physiological response in plant tissue

中村, 純也

https://doi.org/10.15017/1807122

出版情報：九州大学, 2016, 博士（農学）, 課程博士
バージョン：

Analysis of the spatially-resolved metabolic distribution for unraveling the physiological response in plant tissue

Junya Nakamura

Kyushu University

2017

TABLE OF CONTENTS

Acknowledgements

This study was promoted under enthusiastic encouragements and valuable advices from my leaders. I would like to express my gratitude to Professor Hiroyuki Wariishi in Metabolic Architecture Design Laboratory, and Associate Professor Hirofumi Ichinose in Bioresources Chemistry Laboratory. I am also deeply grateful to have a lot of suggestions from Professor Hirofumi Tachibana in Food Chemistry Laboratory, and Associate Professor Yushi Ishibashi in Crop Science Laboratory, and Associate Professor Daisuke Miura, Associate Professor Yoshinori Fujimura, Dr. Tomomi Morikawa-Ichinose in Innovation Center for Medical Redox Navigation, Kyushu University, and Dr. Eisuke Hayakawa in Okinawa Institute of Science and Technology Graduate University. Their assistance was indispensable throughout the study. I also enjoyed good associations with students and staffs in my laboratory. My peaceful life during the PhD course was due to those in close and warm contacts with me. Sincere gratitude is expressed to my family for all the supports I have had. The financial support from scholarship for PhD program student in Kyushu University is acknowledged.

Dedication

To my beloved wife, son, mother and father.

Abbreviations

9-AA	9-aminoacridine
AMP	Adenosine monophosphate
Asp	Aspartate
ATP	Adenosine triphosphate
CMC	Calboxymethyl cellulose
DESI	Desorption electrospray ionization
DHB	2,5-dihydroxybenzoic acid
ESI	Electrospray ionization
GC–MS	Gas chromatography–mass spectrometry
GMOs	Genetic modified organims
Gln	Glutamate
Glt	Glutamine
LC–MS	Liquid chromatography–mass spectrometry
MALDI	Matrix-assisted laser desorption/ionization
MG	Mature green
MS	Mass spectrometry
MSI	Mass spectrometry imaging
MR	Mature red
m/z	Mass to charge ratio
NADPH	Nicotinamide adenine dinucleotide

NMR	Nuclear magnetic resonance
NW	Non-wounded
O.C.T.	Optimum cutting temparature
P stage	Pink stage
Pyr	Pyruvate
Q	quadrupole
QqQ	Triple quadrupole
SA	Sinapic acid
SIMS	Secondary ion mass spectrometry
TCA cycle	Tricarboxylic acid cycle
TOF	Time-of-flight
UDP-Glu	UDP-glucose

List of Tables Page

List of figures Page

Chapter 1.

Recent advances in metabolome research

in living organisms

1.1. Significance of metabolomic analysis for living organisms

1.1.1. Definition of metabolite and metabolism

Metabolites are low-molecular-weight compounds and indispensable components produced during metabolism in living organisms. The substrates are chemically converted to maintain homeostasis through various biochemical activities, such as energy production, and signal transduction via enzymatic or non-enzymatic reactions. The compounds are categorized as either primary or secondary metabolites and are involved in primary or secondary metabolism, respectively. Metabolism is defined as a chemical or synthesis process where inorganic substances are converted into organic compounds within the cells of organisms. Metabolism provides energy, converting nutrition into precursor materials to contain the body, and synthesizing or resolving biogenetic substances, including physiologically active substances, from precursors. Metabolism is usually divided into two categories, substance metabolism, such as catabolism and anabolism, and energy metabolism including chemical, mechanical, and electric forms. In substance metabolism, catabolism plays a key role in the acquisition of energy, such as adenosine triphosphate (ATP) and

nicotinamide adenine dinucleotide (NADPH), through several metabolic pathways, including glycolysis, the tricarboxylic acid (TCA) cycle, and the electron transport chain. In contrast, anabolism includes the synthesis of nucleic acids, proteins, polysaccharides, fatty acids, isoprenoides, and steroids. These types of metabolism are called primary or central metabolism and they form essential pathways for all living organisms.

Secondary pathways of metabolism, such as the synthesis of phenylpropanoids and alkaloids, are specific to some organisms, including plants and selected microorganisms. In general, these compounds are not involved in the normal growth, development, or reproduction of the organisms. Instead, secondary pathways of metabolism play a role in the protection from biotic stresses, such as insects or pests, or from abiotic stresses, including light or temperature.

1.1.2 Definition of metabolome and metabolomics

The metabolome is defined as the set of low-molecular-weight compounds produced in the organism (Oliver S.G. *et al.* 1998) and the metabolomics is a comprehensive analysis

using omics technology to determine the chemical process involving the metabolites (Last R.L. *et al.* 2007). Since the discovery of DNA structure by Watson, Click, and Wilkins, molecular biology techniques have rapidly developed. In the post-genomic era, tremendous efforts have been undertaken to elucidate biological functions. However, understanding biological functions at the molecular level in organisms is still unfinished. Therefore, comprehensive analyses or 'omics' technologies, such as genomics, transcriptomics, proteomics, and metabolomics, are expected to be indispensable for elucidating biological phenomena. The integrative analysis of responses in organisms to a perturbation on the '-omes' levels, such as the transcriptome, proteome, and metabolome, will lead to a better understanding of the biochemical and biological mechanisms in a complex system. However, whereas the technology to study genomics, transcriptomics, and proteomics has significantly advanced, the tools for comprehensive metabolomic analysis are still emerging (Bino R.J. *et al*. 2004).

1.1.3. Analytical significance of metabolites as a "compound-level phenotype"

The formation of a phenotype is influenced by several complicated factors including environmental and genetic components. Understanding phenotypic formation is difficult based solely on the identification of the involved genes or proteins. The studies of genome, transcriptome, and proteome aim to understand the phenotype in living organisms. However, the processes involved in the development of phenotypes are still unclear. In contrast, metabolites are described as the "compound-level phenotype" of genomic information because the molecules are closely related to the phenotype at the substance level (Fig. 1-1). Additionally, metabolites are the result of the interaction of the system's genome and several complicated factors (Rochfort S. 2005). Therefore, metabolomics play a key role as one of the 'omics' technologies to achieve an improved understanding of global systems biology.

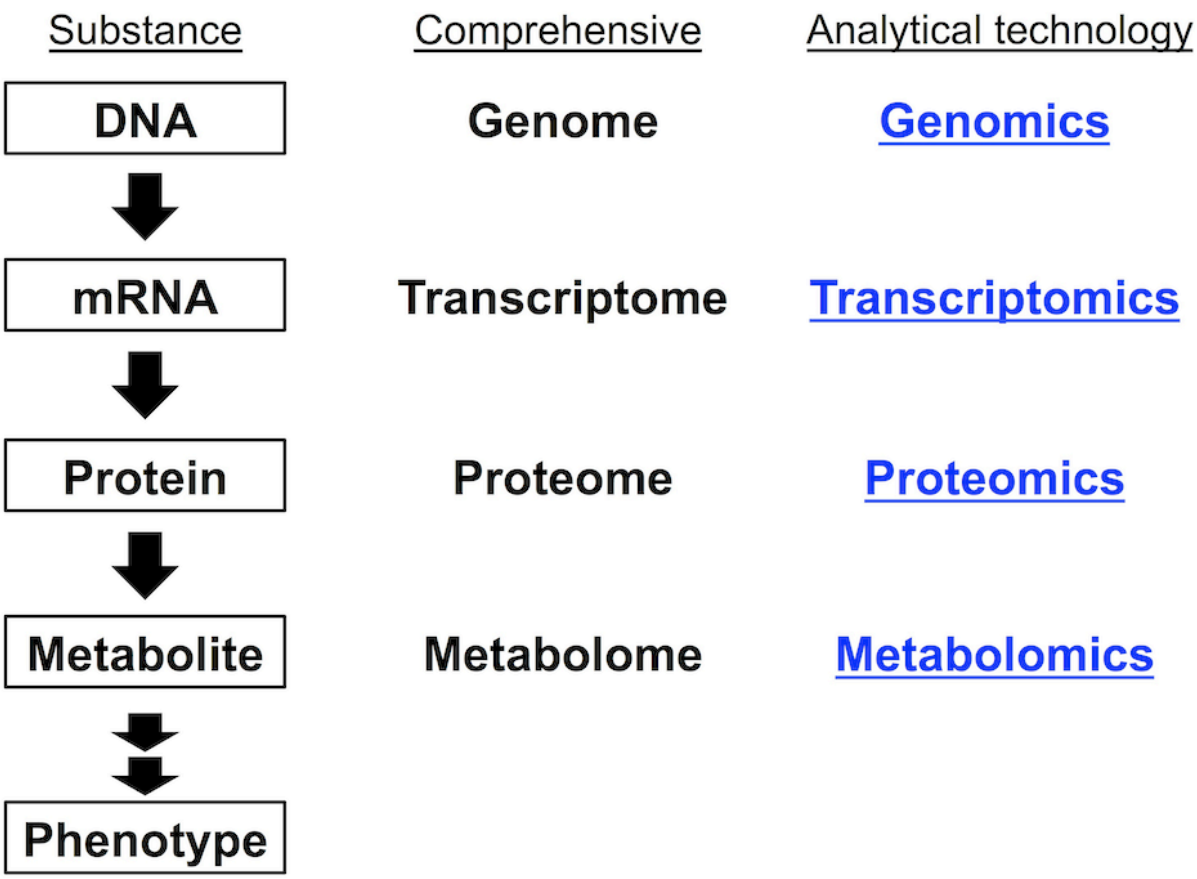

Fig. 1-1 General schematic of 'omics' analysis

1.2. The metabolome in human disease

Diseases are caused by complex interactions among genetic factors, lifestyle, and environmental factors. Understanding the mechanisms of pathogenesis is necessary to obviate the risk of diseases, such as cancer, cerebral vascular disorder, and heart disease. Recent studies have focused on the discovery of biomarkers related to human neurological, immunological, virological, cardiological, and cancer related diseases using a metabolomics approach coupled with mass spectrometry (MS). Early clinical therapy is also closely linked to the discovery of biomarkers using metabolome techniques (Table 1-1). Biomarkers can be identified by examining changes in the concentrations of endogenous metabolites or metabolic flux and correlating the changes with a particular phenotype compared with a control (Nordstöm A. and Lewensohn R. 2010, Liu X. 2016). As an example, Soga *et al*. discovered the ophtalmate biosynthesis pathway using capillary electrophoresis mass spectrometry, a technique suited for the detection of polar and charged compounds (Soga T. *et al*. 2002, 2003, 2006). Therefore, new biomarkers correlated to significant medical illnesses can be identified by metabolomic analysis.

Table 1-1. Applications for human diseases using metabolomics technology

Disease type	Type of sample	Analytical method	Reference
Coronary heart disease	Serum	^{1}H-NMR	Brindle J.T. *et al*. (2002)
Breast cancer	Urine	LC–MS	Frickenschmidt A. *et al*. (2005)
HIV	Serum	^{1}H-NMR	Hewer R. *et al*. (2006)
Fulminant hepatitis	Liver	CE-MS	Soga T. *et al.* (2006)
Huntington's disease	Serum	GC–MS	Underwood B.R. *et al*. (2007)
MMA/PA	Plasma	LC–MS	Wikoff W.R. *et al*. (2007)
Ischemia	Serum	^{1}H-NMR	Barba I. *et al*. (2008)
Colon cancer	Biopsy	GC–MS	Denkert C. *et al*. (2008)
Kidney cancer	Urine	LC–MS	Kim K. *et al.* (2008)

1.3. The metabolome in other research areas

Conventional industrial production based biotechnology used to make vitamins, amino acids, and antibiotics, are produced using microorganisms, including yeast and *E. coli* (Mashego M.R. *et al*. 2007). The emergence of recombinant DNA techniques has led to the specific introduction of the product pathway of interest or enhancement of the product flux naturally produced by the microorganisms (Nielsen J. 2001). However, production rates and the concentrations of target molecules are limited to primary metabolism as primary central carbon metabolism provides precursors, cofactors in the form of NADH and NADPH as well as adenosine triphosphate (ATP). In contrast, metabolomic techniques can help to define the metabolic flux and rate-limiting step. Yukihira *et al*. revealed the dramatic metabolomic dynamics in the primary metabolism in *E. coli* using high-throughput analysis (Yukihira D. *et al*. 2010). Additionally, metabolomics has been applied in the production of alcohol beverages, including beer and sake. For improvement of beer tastes, metabolomics was used to validate the sensory evaluation, stability, and metabolic outputs of a number of yeast strains (Inui T. *et al*. 2013, Heuberger A.L. *et al*. 2012, Pope G.A. *et al*. 2007, Duarte I. *et al*. 2002). In the future, it is expected that food production will become more efficient using metabolome

techniques such as MS coupled to chromatography or NMR spectroscopy.

1.4. The metabolome in plants

Previous studies predicted the number of secondary metabolites in plants to range from approximately 200,000 to 1,000,000 (Fiehn O. 2002, Dixon R.A. and Strack D. 2003, Afendi F.M. *et al*. 2012). Secondary metabolites have unique functions as antioxidants and prevention of illness, such as moon blindness. Recent studies have focused on the modification of metabolism by biotechnological techniques. However, these approaches do not necessarily lead to the expected results. In plants, highly complex regulatory systems control the metabolism. Therefore, more precise information on plant metabolism was needed to elucidate the functions of secondary metabolites.

Investigation of a plant's metabolome can provide comprehensive information of its metabolites. The plant metabolome has been used for the evaluation of genetically modified organisms (GMOs), metabolic quantitative trait loci, and metabolite annotation (Table 1-2). In particular, plant metabolomics is used to evaluate the internationally accepted substantial equivalence in GMOs (Kusano M. *et al*. 2011). Furthermore, understanding of unknown phenomena in the life sciences is expected by applying metabolome technology.

Table 1-2 Applications for plant research using metabolomics technology

Plant speices	Organ	Application	Analytical method	Reference
Arabidopsis	leaf root	Identification of metabolic genes	LC–MS FT–ICR–MS	Tohge T. *et al*. (2005)
Tomato	fruit	Metabolite annotation	LC–FTICR–MS	Iijima Y. *et al*. (2008)
Tomato	fruit	Evaluation of GMOs	GC–MS LC–MS CE–MS	Kusano M. *et al*. (2011)
Tomato	fruit seed	Metabolic quantitative trait loci	GC–MS	Toubiana D. *et al*. (2012)

1.5. Conventional analytical technologies for the study of metabolomics in plants

Metabolomics techniques have become rapidly established because of the development of mass spectrometry coupled with chromatography, such as gas chromatography (GC), liquid chromatography (LC), and capillary electrophoresis (CE), as well as nuclear magnetic resonance (NMR) spectroscopy. In this section, each technique is overviewed in detail.

1.5.1. Nuclear magnetic resonance spectroscopy

Nuclear magnetic resonance (NMR) is a physical phenomenon whereby the atomic nuclei in the magnetic field interact with electromagnetic radiation. NMR spectroscopy has played a key role in the understanding of metabolic dynamics in living organisms for many years (Wishart D.S. 2008). Metabolomic analysis using NMR spectroscopy does not require the samples to be pretreated compared with using MS coupled with chromatography, such as GC–MS and LC–MS. The advantage of the NMR method is that it is non-invasive, highly

quantitative, and enables the identification of complex metabolites. However, the major limitation of NMR for metabolomic analysis is its low sensitivity (Fig. 1-2). However, recent research into the development of cryoprobes, high-strength superconductive magnets and multi-dimensional NMR techniques has helped to overcome this limitation (Kikuchi J. *et al*. 2004, Kovacs H. *et al*. 2005).

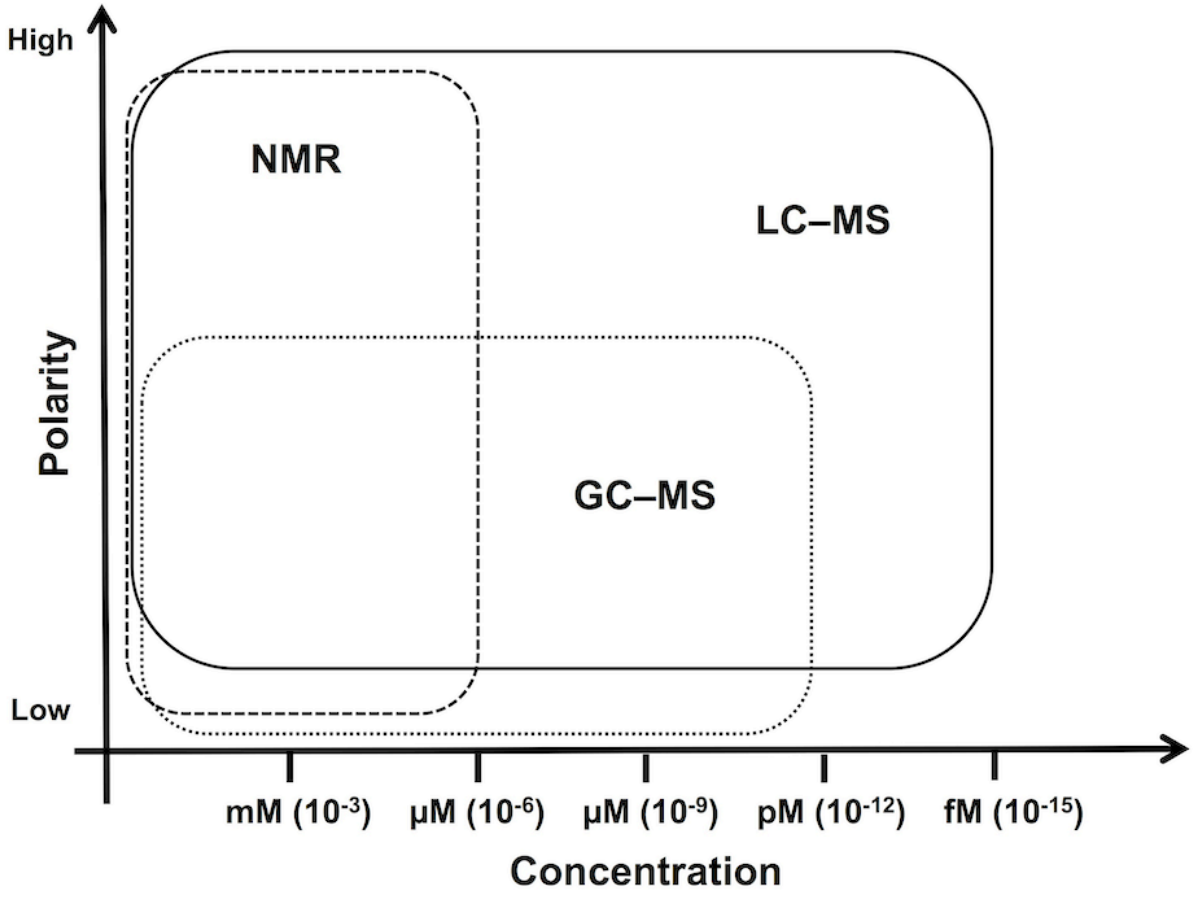

Fig. 1-2 Coverage of metabolite classes with different detection methods

1.5.2. Gas chromatography mass spectrometry

Gas chromatography mass spectrometry (GC–MS) coupled to electron ionization (EI), as shown in Fig. 1-3, is the most commonly used technique in metabolomics to analyze volatiles, such as terpenoids and polar compounds, including sugars, phosphorylated compounds, amino acids, organic acids, and hydrophilic vitamins (Fiehn O. *et al*. 2000, Roessner U. *et al*. 2000, 2001, Okazaki Y. and Saito K. 2012). The fragment ions are obtained by subjecting the compounds to an electric field set at 70 eV because this energy historically leads to reproducible fragment spectra and allows compounds to be identified by comparing the fragments to a mass spectral library (Jonsson P. *et al*. 2005, Kind T. and Fiehn O. 2010, Lei Z. *et al*. 2011, Bouhifd M. *et al*. 2013). Fiehn *et al*. quantified more than 300 distinct compounds from *Arabidopsis* leaf extracts (Fiehn O. *et al*. 2000). Although the method demonstrated innovative performance in metabolomics with GC–MS, it was constricted by the need for multiple derivatization procedures for each chemical moiety, and the fact that non-volatile compounds could not be determined.

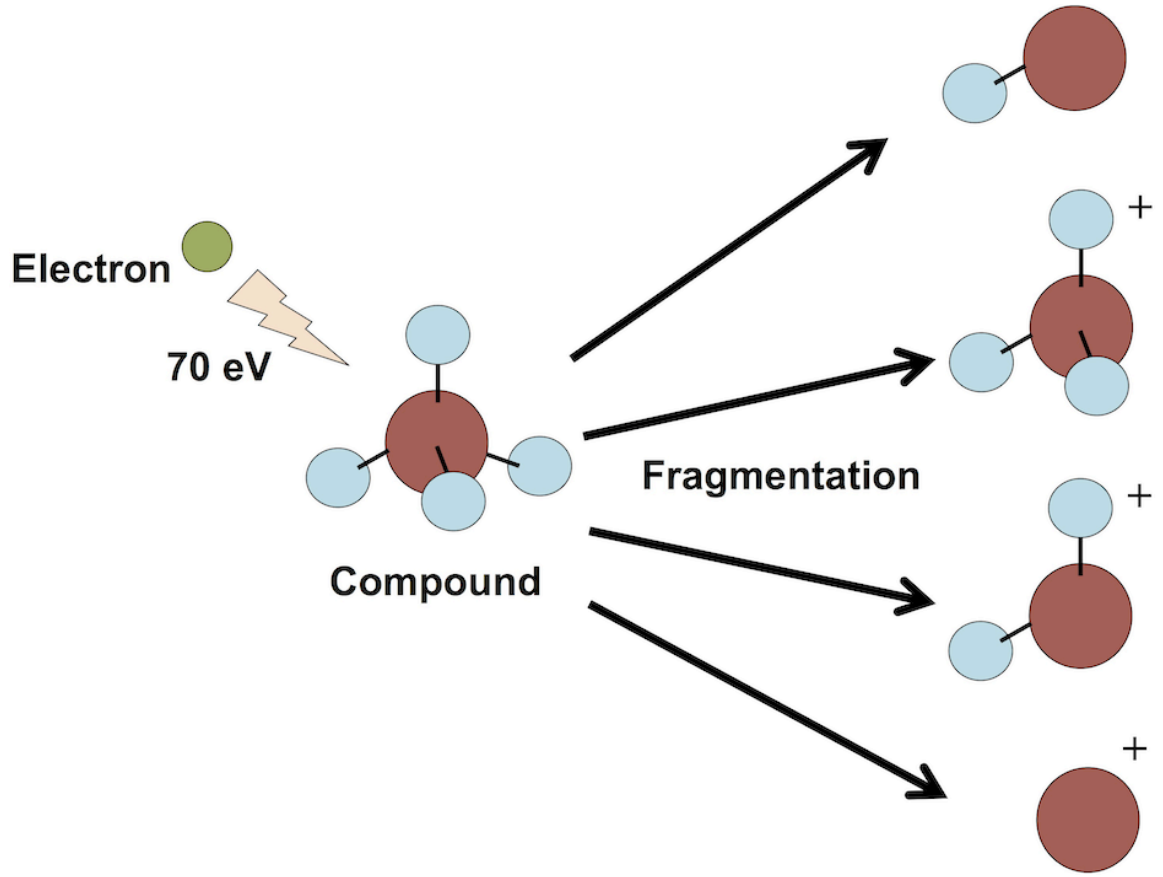

Fig. 1-3 Overview of electron ionization (EI) method

1.5.3. Liquid chromatography mass spectrometry

Liquid chromatography mass spectrometry (LC-MS) combined with atmospheric ionization, which includes electrospray ionization and atmospheric chemical ionization, is also used for metabolomic research (Fig. 1-4). LC-MS analysis is suited for compounds with chemically categorized unstable functional groups or high vapor points. The method is also useful to detect thermolabile, polar metabolites without any derivatization steps. In plant metabolomics, LC-MS is often used to detect the secondary metabolites, including phenylpropanoids and alkaloids, with a reversed-phase column, such as C18, for the separation step (Matsuda F. *et al*. 2009, 2010, Tohge T. and Fernie A.R. 2015). Furthermore, the introduction of MS instruments with time-of-flight and triple quadrupole capabilities, coupled with LC has enabled the detection of metabolites with high sensitive and mass accuracy (Pyke J.S. *et al*. 2015). The use of LC-MS in plant metabolomics is limited by the occurrence of ion suppression that results from the co-elution of interfering compounds present in the complex matrix (Choi B.K. *et al*. 2001, Matuszewki B.K. *et al*. 2003, Trufelli H. *et al*. 2011). The existence of multiple compounds affects the ionization and transfer of analytes from the liquid to the gas phase and potentially compromises the accurate

quantification of low-molecular-weight compounds (Wilson I.D. and Brinkman U.A.T. 2003). Optimization of the chromatographic separation is important to reduce the impact of matrix effects in the mass spectrometer. Matrix effects can be avoided by adding a known amount of an internal standard in the plant extract at the beginning of the extraction procedure (Fernie A.R. *et al*. 2004, Antonio C. *et al*. 2007, Burton L. *et al*. 2008). Another limitation of LC-MS target metabolite analysis is that reference compounds are needed for identification. In contrast, application of the seven golden rules or the use of databases for identification of metabolites will help to overcome this issue (Kind T. and Fiehn O. 2007, Ruttkies C. *et al*. 2016).

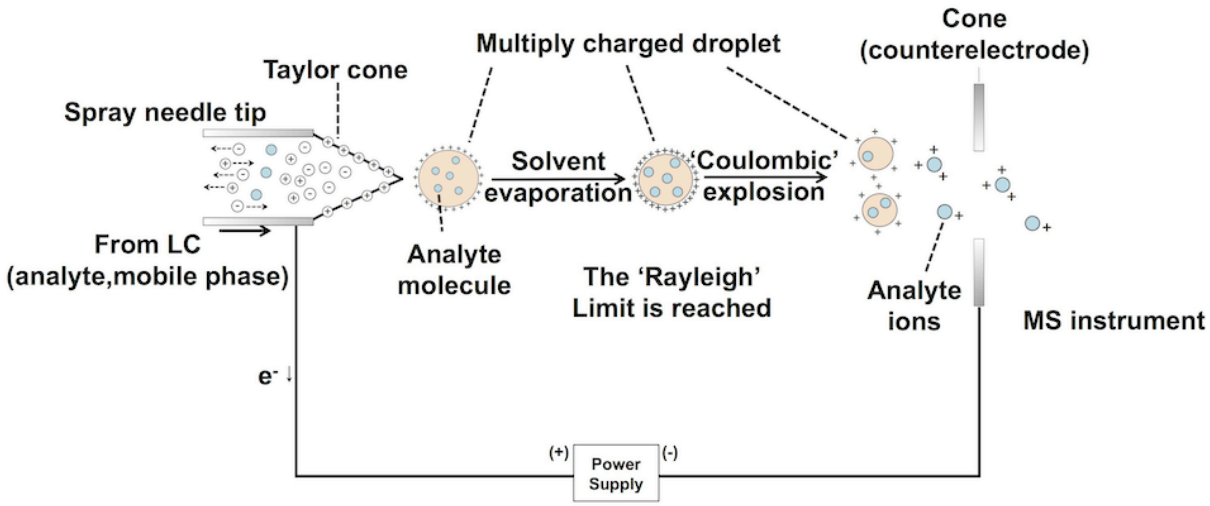

Fig. 1-4 Overview of electrospray ionization (ESI) method

Table 1-3 Advantages and disadvantages of metabolomic analytical method

Method	Advantages	Disadvantages
Nuclear magnetic resonance (NMR) microscopy	- Non-invasive - High temporal resolution	- Less sensitive than mass spectrometry
Gas chromatography mass spectrometry (GC–MS)	- High sensitivity - Conditioned compounds library	- Needs to derivatization - Destructive to sample
Liquid chromatography mass spectrometry (LC–MS)	- High sensitivity - No derivatization step	- Destructive to sample - Difficulty of compound identify

1.6. Sample preparation and data analysis

1.6.1. Sample preparation

In the analytical sciences, the quality of the sample preparation directly influences the data. In general, fresh or frozen plant samples are quantitated before the extraction step. Sample extraction is an important step in the sample preparation. A common extraction solvent for the separation of polar and non-polar metabolites is a two-phase solution of chloroform, methanol, and water (2:1:1, v/v).

1.6.2. Mass spectrometry data format

A number of MS data formats exist. Open-access file formats, such as ASCII, and XML, were developed as a result of the efforts of several bioinformatic researchers. Recently, an mzXML format has become widely accepted although it does not contain biological descriptive information. The use of a XML format for metabolomic analysis provides standardization of the quantitative data output. Additionally, the format is suitable for the

sample annotation to biological interpretation of the obtained data.

1.6.3. Data extraction

Raw data derived from the sample are stored as a series of mass spectra acquired at a given time point or scan. Every scan is represented by a set of mass-to-charge (*m/z*) and intensity vectors. In metabolomic analyses, these data are necessary to align all information, including *m/z*, and retention time. Additionally, the data needs to be outputted as a uniform matrix to compare the control with the treatment data. In this step, binning is sometimes required to reduce the extraction information and convert the continuous mass spectra into a centroid format. When the vectors of mass intensity data are converted to a uniform length, the dataset can be expressed as a matrix ($m \times s \times f$, *m;* the length of mass vector, *s*; the retention time, f; the number of files) (Dettmer K. *et al*. 2007).

1.6.4. Normalization

After data processing, normalization is required to remove the systematic bias in ion intensities between measurements while retaining the biological variation. In general, the chemical diversity of metabolites that leads to different recoveries during extraction or responses during MS ionization makes it difficult to separate the interesting biological variation from the undesired systematic bias. Strategies for normalization of metabolomic data can be divided into two major categories, normalization by unit norm or median intensities, or the maximum likelihood method and normalization by a single or multiple internal external standards based on empirical rules, such as specific regions of retention time.

1.6.5. Statistical analysis techniques for metabolomic data

The methods of analysis for metabolomic data have often modified the transcriptomics analysis. Conventional data analytical approaches attempt to evaluate group-wide differences using univariates, including the t-test and analysis of variance (ANOVA), or multivariate

techniques, such as principal component analysis (PCA) and partial least squares regression (PLS). However, these methods make it difficult to discriminate between experimental categories if only minor differences exist at the single compound level, even though multi-compound combinations would delineate them on a system level. Therefore, multivariate analysis, such as PCA and PLS, are needed to identify not only single compound changes between different experimental groups, but also to use the dependency structures between the individual molecules. PCA and PLS are the most prominent multivariate analysis used in the field of metabolomics.

PCA uses an unsupervised linear mixture model to explain the variance within a dataset by a small number of mutually independent principal components (PCs). These PCs are expressed as vectors of the low-molecular-weight compound contributions in the metabolomic data. All of the factors are considered such that they are paired orthogonal to each other and ordered by the amount of variance they explain. PCA can be interpreted as a linear mixture model and the data matrix is factorized into two matrices. PCA is often used in a hypothesis free exploratory experiment because the method enables dimensional reduction. Additionally, this technique also provides clustering and discrimination of the sample group.

PLS regression, a supervised linear mixture model, is used to recognize an optimal

discrimination of the predictor dataset given a matrix of responses. In particular, PLS-discriminant analysis (PLS-DA) associates the data matrix to the response vector containing the sample class affiliations using a linear regression model. PLS-DA is often utilized to purpose the classification to extract the variables maximizing the discrimination between predefined sample groups or to predict affiliations of an unknown class of samples based on a calibration set of classified distributions. Furthermore, the orthogonal-PLS (OPLS) is also a PLS method. The major difference to conventional PLS analysis is to divide the data variation into the variance of interest, related to the response, and an orthogonal part, unrelated to the response. This leads to a simplified interpretability of the obtained components permitting one to additionally evaluate variance within and between groups. OPLS is a remarkable type of data analysis in the field of metabolomics with a broad variety of classification methods (Bartel J. *et al*. 2013).

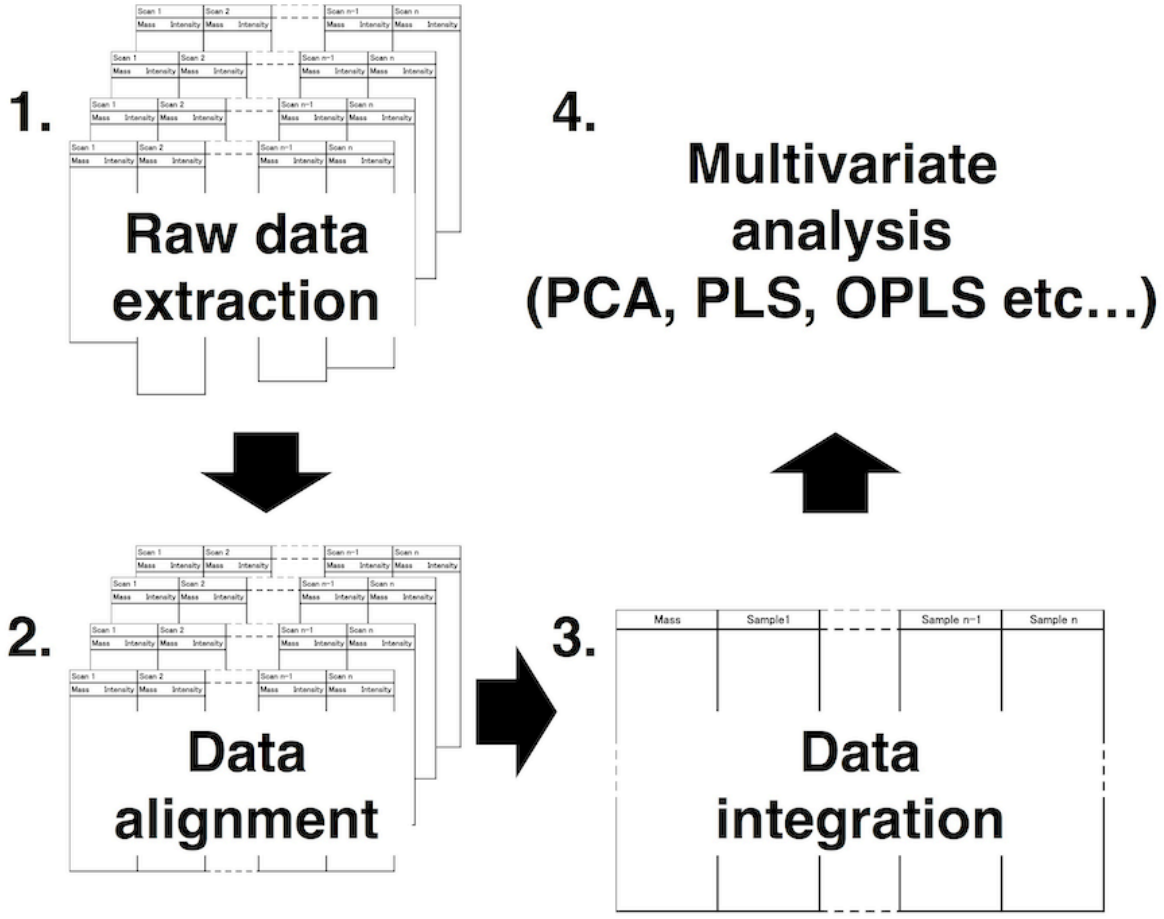

Fig. 1-5 Overview of the data analysis for the metabolomic research

1.7. Concluding remarks

Metabolomics is a powerful approach to obtain comprehensive metabolomic data to understand the physiological responses in living organisms. Conventional metabolomic analysis is often used in NMR spectroscopy and MS coupled to chromatography, such as GC-MS and LC-MS. These methods provide new perspectives on the elucidation of the life phenomenon in organisms. However, although these methods are coupled with ideal data analysis approaches, they require metabolite extraction, which results in the loss of information on the spatial distribution of the metabolites. Therefore, spatial information at each metabolite concentration is required to elucidate the local phenomenon occurring in the tissue.

Chapter 2.

Introduction to the analysis of the distribution of metabolites in plants using imaging techniques

2.1. Significance of metabolite imaging for plant biology

Conventional metabolomic analyses using MS instruments coupled to chromatography, such as GC-MS, and LC-MS are attractive for profiling the comprehensive metabolic behavior in plant tissues (see Chapter 1). Additionally, previous studies predicted that there are numerous secondary metabolites in plants ranging from approximately 200,000 to 1,000,000 in plants (Fiehn O. 2002, Dixon R.A. and Strack D. 2003, Afendi F.M. *et al.* 2012). The compounds play key roles in maintaining homeostasis, such as protection from ultraviolet damage and pest invasion although they are not essential for fundamental metabolism, such as growth and development. However, the function of most secondary metabolites is still unknown in plants or in the human diet because secondary compounds also have complex chemical structures generated by the precise regulation of biosynthetic enzymes. However, conventional metabolomic analytical techniques, MS coupled to chromatography, have limitations in terms of the sample preparation because of the requirement for metabolite extraction, which results in the loss of information on the spatial distribution of the metabolites.

Imaging techniques with invasive and non-invasive methods of sample preparation do not

require the metabolic extraction step. Therefore, the technology has been rapidly developed to assess local metabolic changes or responses in plant materials. Previous studies had used invasive techniques, such as nuclear magnetic resonance (NMR) imaging and Raman microspectroscopy. In contrast, non-invasive imaging technologies, including desorption electrospray ionization (DESI), secondary ion mass spectrometry (SIMS), and matrix-assisted laser desorption/ionization mass spectrometry imaging (MALDI-MSI) is often used to investigate physiological responses.

2.2. Non-invasive metabolite imaging

Spatial information of metabolite distribution is needed to elucidate its local response in tissue. In particular, imaging techniques that can be used to determine the spatial information of biomolecules is an attractive method.

2.2.1. Nuclear magnetic resonance imaging

NMR imaging is an attractive technique for visualizing the spatial distribution of molecules in living organisms. The technique is commonly used for whole body applications in clinical research and diagnostics. NMR imaging is a non-invasive method and can be used to observe time-dependent changes in organisms. Additionally, it can be used to obtain the information normally provided by NMR experiments, including a wide range of chemical and physical properties. In the plant science, ^{1}H-NMR imaging is often used because the hydrogen nuclei found in water molecules represent a major source of sample magnetization. Recently, the distribution of total lipids, a low-molecular-weight compound, is visualized using this

method in an effort to unravel the mechanisms of storage in plant organs, including the seed (Neuberger T. *et al.* 2008, Horn P.J. *et al.* 2012, 2013). However, NMR imaging cannot be used to determine the information on the spatial distribution of specific molecular compositions.

2.2.2. Raman microspectroscopy

Raman microscopy, a type of chemical imaging, is also a nondestructive technique used to visualize spatially resolved chemical information. The method involves monitoring molecular vibrations and depends on inelastic scattering with a photon from a laser light source. Generally, the molecular categories are defined from the Raman shift. For example, the scattering intensities between 2,800 and 3,100 cm^{-1} originate from C–H stretching vibrations. For example, the distribution of lipids and proteins was visualized in nematodes such as *Caenorhabditis elegans* and *Radopholus similis* using Raman spectroscopy combined with optical microscopy (Klapper M. *et al.* 2011, Hölscher D. *et al.* 2014). The distribution of lipids and proteins was easily visualized because they were abundant in these organisms. In

contrast, the distribution of molecules existing at only low concentrations could not be visualized using this technique because the Raman peaks overlap with the peaks derived from other biomolecules and the compound distribution was not clearly visualized. However, the distribution of cytochrome c, carotenoids, and chlorophylls, existing at low concentrations in the cells, was easily visualized because these compounds strongly absorb light and they show resonance Raman scattering.

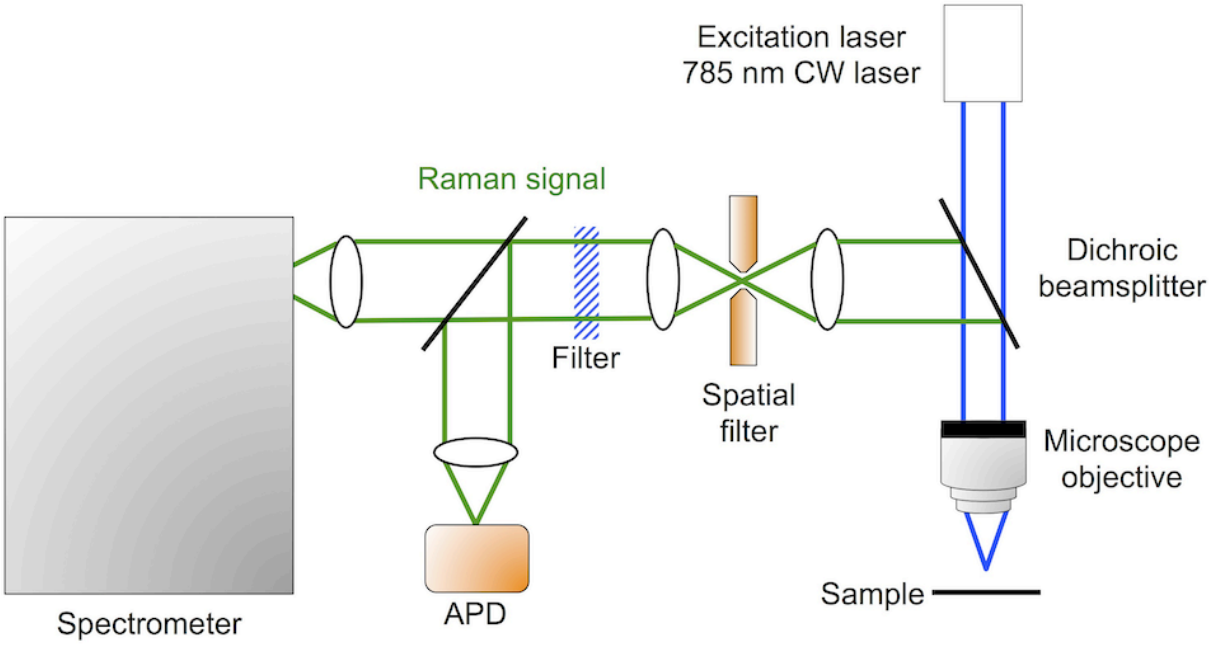

Fig. 2-1 Overview of Raman microspectroscopy

2.3. Mass spectrometry imaging

The distribution of biomolecular species, such as lipids and proteins, in plants has been visualized by non-destructive methods, including Raman microspectroscopy and NMR imaging. In contrast, mass spectrometry imaging (MSI) techniques coupled with desorption electrospray ionization (DESI), secondary ion mass spectrometry (SIMS), and matrix assisted laser desorption/ionization (MALDI), are very useful technologies for determining the distribution of biomolecular species although they are invasive methods.

2.3.1. Desorption electrospray ionization

Desorption electrospray ionization (DESI) is a novel method of desorption/ionization that allows the analysis of the surface without the matrix, material enhanced ionization, or other treatments under ambient conditions (Takáts Z. *et al.* 2004, Fig.2-2). The method utilizes an aqueous spray and the application of a nebulizer gas with a high voltage, resulting in a beam of charged droplets. Recently, DESI-MSI has been performed using an indirect approach on

an insulating surface, such as porous polytetrafluoroethylene (Thuning J. *et al.* 2011). Using this method, distribution of several lipid species was visualized using an animal brain (Wiseman J. M. *et al.* 2006). The method has several drawbacks for applications in plant research. Plants have layers of cuticles and it is difficult for the DESI spray to penetrate the layers to access the biomolecules in plant organs. Recently, some researchers used cross-sections on glass slides to overcome this problem and visualized a heterogeneous distribution of hydroxynitrile glucosides in cassava (*Manihot esculenta*) tubers (Li B. *et al.* 2013). However, the spatial resolution is only approximately 200 μm. Therefore, ion-imaging data with resolutions more than 200 μm cannot be acquired using DESI-MSI.

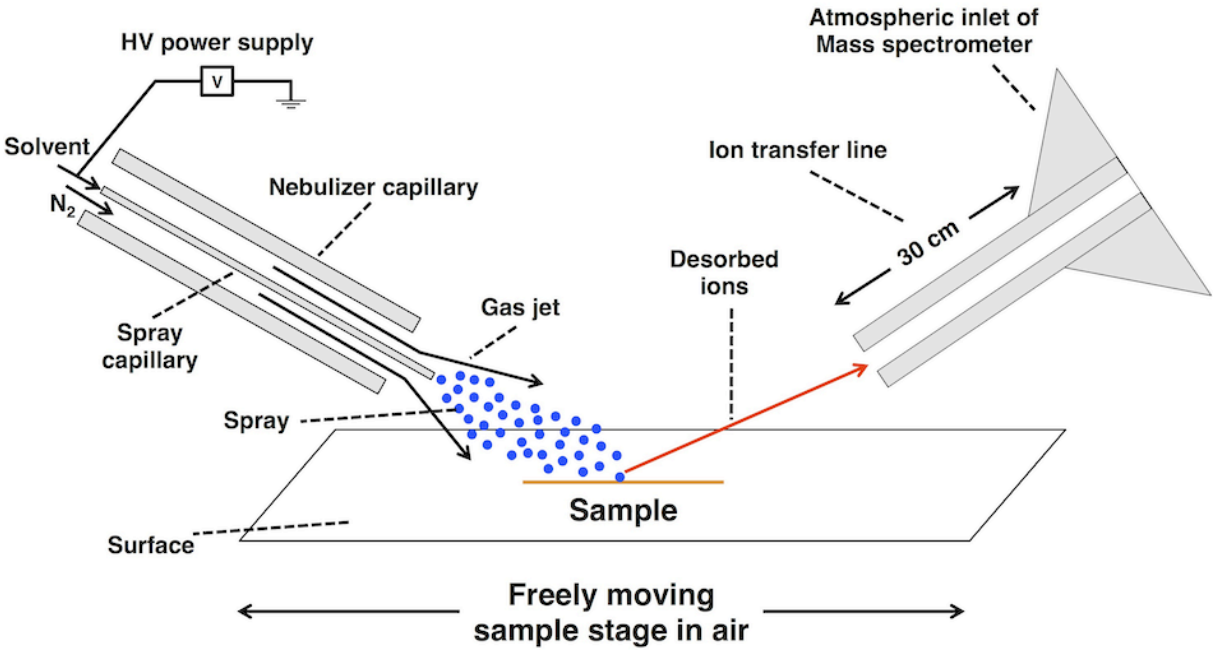

Fig. 2-2. Schematic of DESI experiment

2.3.2. Secondary ion mass spectrometry

Unlike other MSI experiments, TOF secondary ion mass spectrometry (SIMS) imaging can be used to obtain the distribution of low-molecular-weight compounds, such as metabolites and lipids, with high spatial resolution under a high vacuum condition (Geurquin-Kerm J.L. *et al.* 2005). Laprévote et al. characterized the distribution of flavonoids in wild-type *Arabidopsis* (*Arabidopsis thaliana*) seed and several varieties of pea (*Pisum sativum*) seed using an optimized method of sample preparation and TOF-SIMS spectrometry (Seyer A. *et al.* 2010). One advantage of SIMS over other MS methods, such as DESI and MALDI, is that it allows high spatial resolution (> 100 nm) to be obtained. However, its use for imaging of plant tissue is very limited because SIMS operates under a high vacuum condition and uses highly energetic primary ions (5–40 keV), although several researchers have employed TOF-SIMS for plant tissue imaging.

2.3.3. Matrix-assisted laser desorption/ionization mass spectrometry imaging

The matrix-assisted laser desorption/ionization mass spectrometry imaging (MALDI-MSI) technique was first reported by Caprioli *et al.* to generate ion images from the samples as mass-to-charge (*m/z*) values (Caprioli R.M. *et al.* 1997). Recently, the use of MALDI-MSI is increasing in fields such as agricultural and pharmacological sciences although other analytical technologies, including DESI-MSI and TOF-SIMS-MSI have been developed. In this section, the MALDI-MSI experiment is highlighted as a method used to understand the physiological responses in plants.

2.3.3.1. Sample preparation for matrix-assisted laser desorption/ionization mass spectrometry imaging experiments

In MALDI-MSI experiments, sample preparation is critical to obtaining high quality data. A thin-section of sample is needed to efficiently detect the signal and obtain high signal quality in terms of peak intensity and signal-noise ratio (S/N) (Sugiura Y. *et al.* 2006).

Generally, a thin section of 10–20 μm of plant tissue was prepared for MSI (Zaima N. *et al* 2010, Yoshimura Y. *et al.* 2012). There are a number of materials for embedding the sample, such as O.C.T. compound, carboxymethyl cellulose (CMC), and ice. The Kawamoto method (Kawamoto T. 2003) has also been used to prepare hard samples, including cereal grains (Zaima N. *et al.* 2010). In contrast, when fruit tissue was prepared in thin sections without any embedding materials, the shape of each organ structure was maintained (see Chapter 3). Furthermore, Shroff et al. used Arabidopsis leaves without sectioning and visualized the distribution of glucosinolates using MALDI-MSI (Shroff R. *et al.* 2008, 2015). Therefore, it is necessary when choosing the sample preparation method for MALDI-MSI analysis, the type of plant tissue should be taken into account.

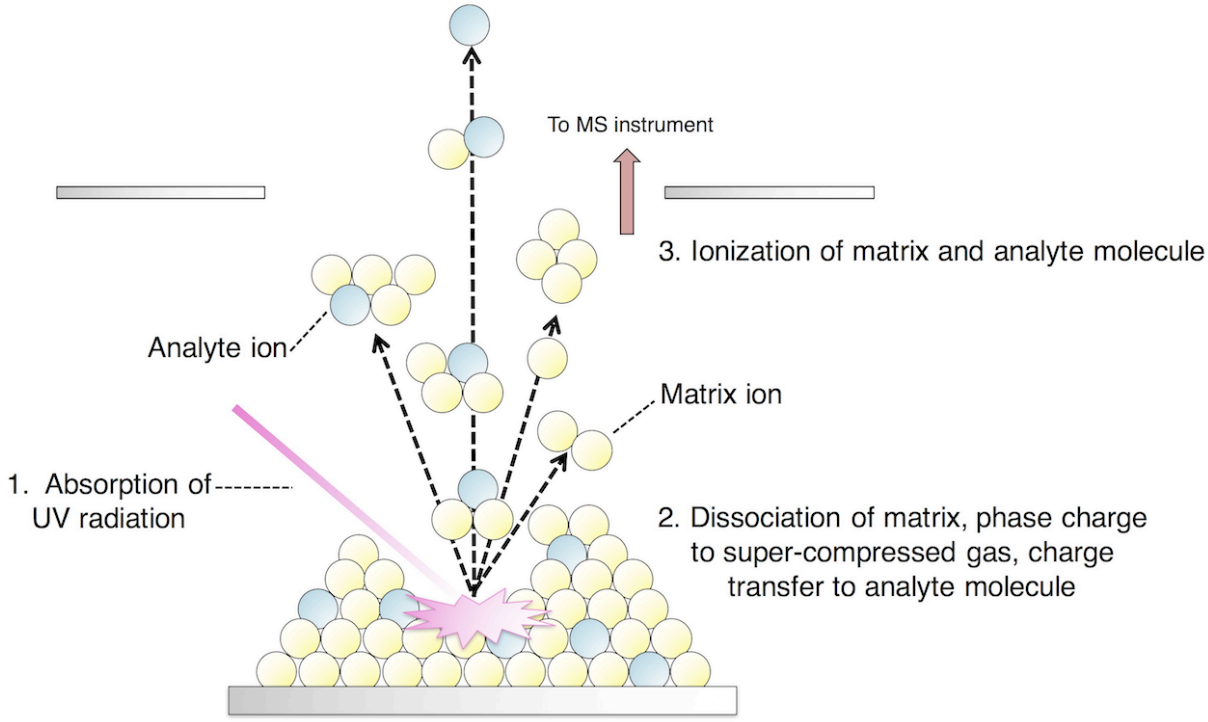

Fig. 2-3 Overview of matrix-assisted laser desorption/ionization (MALDI) method

2.3.3.2. Matrix selection

The choice of matrix is important for metabolite imaging. Previous MALDI-MSI reports have used conventional matrices, such as 2,5-dihydroxybenzoic acid (DHB), α-cyano-4-cinnamic acid, and sinapic acid (SA) in positive ionization mode. These matrices can be used to detect abundant molecules in the sample tissue, such as proteins, peptides, and lipids (Sugiura Y. *et al.* 2008, Shimma S. *et al.* 2008, Grassl J. *et al.* 2011). However, these matrices are not suitable for analyzing low-molecular-weight compounds because of the detection of multiple peaks derived from the matrix in the low-mass range ($m/z < 700$). In contrast, the use of 9-aminoacridine (9-AA), a matrix that exhibits few peaks in the low-mass range, allows the detection of trace amounts of metabolites belonging the low-molecular-weight-compounds with high sensitivity in thin sample sections (Miura D. *et al.* 2010, Yukihira D. *et al.* 2010). Using a 9-AA-MALDI-MSI system, we simultaneously visualized the distribution of multiple primary metabolites such as amino acids, phosphorylated sugars, and nucleotides (Miura D. *et al.* 2010). In contrast, 1,5-diaminonaphthalene (1,5-DAN)-based MALDI-MSI was used to visualize epigallocatechin-3-*O*-gallate (EGCG), the major bioactive green tea polyphenol, and its phase

II metabolites with high sensitivity (Kim Y.H. *et al.* 2013). However, the mechanisms of ionization in MALDI are still unclear. To effectively ionize biomolecules in MALDI-MSI, the selection of the matrix is one of the most important steps. Recently, a quantitative structure–property relationship (QSPR) analysis was performed to model an experimental evaluation using *in silico* molecular descriptors of low-molecular-weight compounds (Yukihira D. *et al.* 2013).

2.3.3.3. Matrix deposition

In MALDI-MSI, the matrix is commonly deposited using a spray-coating method and an airbrush because it is simple and convenient. Distribution of several unique metabolites using various plant materials, including Arabidopsis leaves, blueberry, and rice grain was visualized using a spray-coating method by MSI (Shroff R. *et al.* 2008, Zaima N. *et al.* 2010, Yoshimura Y. *et al.* 2012). However, the technique requires manual operation, and the quality of the resultant sample is completely dependent on the skill of the operator. In particular, poor reproducibility is a critical issue that can hamper data acquisition (Germperline E. *et al.* 2014).

In contrast, sublimation coupled with a recrystallization method can be used under atmospheric or vacuum conditions. Use of a sublimation method was previously reported to be suitable for the detection of several glucosinolates in *Arabidopsis* leaves (Shroff R. *et al.* 2015). This method can be performed by automated equipment and minimizes human errors. Furthermore, the sublimation method is more suitable for high spatial resolution imaging compared with the spray-coating method (Hankin J.A. 2007). However, the two methods provided different coverage and sensitivity of detectable metabolites (Gemperline E. *et al.* 2014). Therefore, ultimately researchers must select the matrix deposition method most suitable for detecting the metabolites of interest.

2.3.3.4. Data analysis

Acquired MALDI-MSI data are processed with a freely available software Biomap (http://ms-imaging.org.) or other software. The software is used for the creation of a two-dimensional ion-density map, normalization of peak intensity, adjustment of the color scale, and quantification of the ion intensity. In contrast, MSIdV can be used to create ratio

map imaging, such as energy charge ratio imaging, in some steps using the binary files of imzML-formatted files (Hayakawa E. *et al.* 2016). Additionally, a metabolite derived from a sample tissue section is identified and/or estimated by comparing with a standard compound or the information available in public databases such as Mass Bank, METLIN and the Human Metabolome Database. Therefore, compounds that are not available as standards and/or do not have their fragment spectra tabulated in the databases are difficult to identify in the MSI experiment. Additionally, it is thought that MS spectra may include fragment peaks derived from the metabolite in the MSI experiment. Thus, further research will be required to strategically identify metabolites through their fragment spectra and coordinate each compound category with the MS/MS spectra obtained from the metabolites derived from the sample tissue section in the MSI experiment.

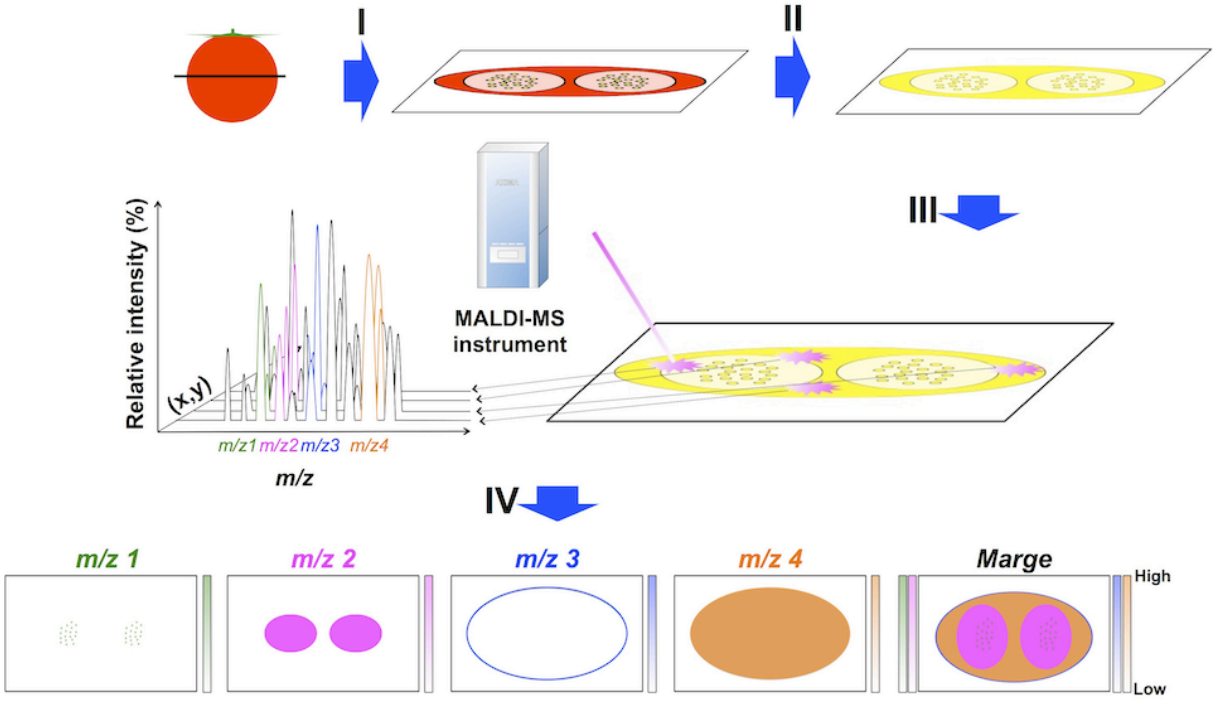

Fig. 2-4 Schematic of MALDI–MSI experiment. I. Cryosectioning and thaw-mounting on conductive slide glass. II. Matrix application and/or recrystallization. III. MALDI-MS analysis. IV. Reconstruction of ion image

2.4. The aim of this study

In this chapter, metabolite imaging for plant biology will be discussed with a focus on the advantages and disadvantages of recent imaging technological advances. The MALDI-MSI technique is a remarkable new technology useful to obtain spatiotemporal metabolomic information, although there are a number of excellent analytical technologies. Information on spatiotemporal metabolic behavior is indispensable for a precise understanding of physiological response, but such information is still limited. Here, we attempt to determine the spatial distributions of multiple primary and secondary metabolites simultaneously within tissue sections of tomato fruit using a MALDI-MSI technique.

Chapter 3.

Spatially-resolved metabolic distribution for unraveling the physiological change and responses in tomato fruit using MALDI-MSI

3.1. Introduction

Endogenous metabolites are important components related to fruit phenotypes, such as color, flavor, taste and texture. Their concentrations will dramatically and spatiotemporally change during growing and ripening processes (Alexander L. and Gerierson D. 2002, McAtee P. *et al*. 2013, Osorio S. *et al*. 2013). Both biotic and abiotic stresses also trigger concentration changes, which lead to whole-tissue physiological changes, such as alterations in color and taste during the ripening process, or more local and partial responses, such as morphological changes induced by wounding and pest-associated stresses (Saltveit M.E. 2000, Baldassarre V. *et al*. 2015). These events are strictly regulated, and alterations in metabolic dynamics occur as the result of a wide range of biochemical processes, including enzymatic or non-enzymatic reactions (Zanor M.I. *et al*. 2009, Osorio S. *et al*. 2011, Baldina S. *et al*. 2016).

The metabolome closely represents the phenotype of an organism under a given set of conditions and is defined as the "compound-level-phenotype" of the genomic information. Metabolomics is an effective approach for understanding global metabolic changes in fruit (Kusano M. *et al*. 2011). This approach allows for the quantitative determination of each metabolite and for tracing metabolic regulation in tissues during ripening and wounding stress.

It can reveal potential relationships between metabolic signatures and phenotypes, such as physiological appearance and functional characteristics. These findings enhance the understanding of physiological mechanisms in the fruit, and this approach is expected to contribute to plant breeding and postharvest technology, such as food preservation and processing. Conventional metabolomics uses gas chromatography-mass spectrometry (GC–MS) and liquid chromatography–MS (LC–MS) to detect various metabolites, which appear at average levels, simultaneously in whole tissues. However, these methods do not address the spatial aspects of more local physiological phenomena, such as metabolic responses against wounding or pest stress at tissue micro-regional levels. Information on spatiotemporal metabolic behavior is quite important to precisely understand physiological changes and responses related to the tissue micro-regions of the functional compartments in fruit.

Matrix-assisted laser desorption/ionization–mass spectrometry imaging (MALDI–MSI) is a new remarkable technology (Caprioli R.M. *et al*. 1997, Stoeckli *et al*. 2001, Miura D. *et al*. 2012). This technique determines the spatial distribution of biomolecules, such as low-molecular-weight compounds, metabolites, proteins and peptides, in tissue at a high spatial resolution without any labeling. Metabolite distributions were reported in several plant

tissues, such as blueberry, cereal grains and Arabidopsis (Yoshimura Y. *et al*. 2012, Zaima N. *et al*. 2010, Shroff R. *et al*. 2015). However, sample preparation methods were different among plant tissues, and no observations focused on more local physiological responses in the tissue. Tomato (*Solanum lycopersicum* L.) fruit is an edible horticultural crop that is highly consumed worldwide and is used as a model plant of maturation (Alexander L. and Grierson D. 2002). Studies of tomato fruit, focused on understanding highly-resolved metabolic behavior, are expected to unravel basic mechanisms of physiological changes and responses, as well as morphological alterations. However, the MALDI–MSI technique has not yet been applied in tomato fruit research. Here, we succeeded in determining the spatial distributions of multiple primary and secondary metabolites simultaneously within tissue sections of mature red (MR) tomato fruit using MALDI–MSI technique. Their unique localizations were observed in distinctive tissue compartments, such as mesocarp and locule regions. To investigate whole physiological changes at the metabolite level in the tomato fruit, metabolite distributions were compared using two different samples, mature green (MG) and MR tomato fruits. Furthermore, we assessed more local metabolic changes in tomato fruit during the ripening process after wounding, using MG as a control for the beginning stage of ripening and the pink stage (P) fruit, corresponding to the mid-stage. The wounded (W) fruit

was prepared by wounding MG and at ripening stage up to the P. We compared the difference between MG and P to determine the metabolic changes occurred from the beginning to the mid-stage of ripening. Additionally, we investigated wound-specific metabolic alterations using the two types of P fruits between non-wounded (NW) and W. The MALDI–MSI technique enabled us to investigate large-scale and more local physiological responses of tomato fruit by detecting spatiotemporally-resolved metabolic behaviors.

3.2. Materials and methods

3.2.1. Materials

Indium thin oxide (ITO)-coated slide glass was obtained from Matsunami Glass (Osaka, Japan). A matrix, 9-aminoacridine (9-AA), was purchased from Merck (Kenilworn, NJ, USA). Another matrix, 2,5-dihydroxybenzoic acid (DHB), and the organic solvents, internal standards and metabolite standards were also obtained from Wako Pure Chemical Industries (Osaka, Japan).

3.2.2. Preparation of tomato (*Solanum lycopersicum* L.) fruit

Tomato (*Solanum lycopersicum* L. ver. Chika) fruits were produced in Sotetsu horticultural farm (Kumamoto, Japan). We purchased both the mature green (MG) and mature red (MR) tomato fruits. MG and MR fruits were harvested at around 35 and 45 days after pollination, respectively. The wounded (W) sample was prepared by wounding MG fruits

with the stainless blade. The wounding width was 5.0 mm and the depth was 1.0 mm. Both W and non-wounded (NW) samples were incubated on the room temperature for one week under non-sterile condition. Both W and NW samples were the same pink-stage fruits, corresponding to the mid-stage, in which less than 60% of the pericarp had changed from green to red during the ripening. All tomato fruits were stored at -20˚C.

3.2.3. MALDI–MSI analysis of the tomato fruit section

The tomato fruit tissues were sectioned at 10 μm thickness using a cryomictorome, and then the sections were thaw-mounted onto ITO-coated glass slide. In this process, we used the optical cutting temperature (O. C. T.) compound for directly mounting the whole tomato fruit on the stage of the cryomictorome. For 9-AA-based MALDI–MSI experiment, matrix (9-AA) was sublimated using iMLayer (Shimadzu, Kyoto, Japan), a sample preparation device which can monitor temperature and matrix deposition thickness during the sublimation. The powder of 9-AA (600 mg) was sublimated at 220˚C under vacuum conditions (5×10^{-2} Pa) and the thickness of matrix was monitored at 0.5 μm. After sublimation, 10% methanol was vapored

to promote both extraction of metabolites from tissue and recrystallization at 60˚C for 3 min (Yang J. and Caprioli R.M. 2011). For DHB-based MALDI–MSI experiments, matrix solution (20 mg/mL DHB in methanol containing 0.1% trifluoroacetic acid (TFA, v/v)) was sprayed with an airbrush in draft hood under room temperature. After matrix deposition, samples were subjected to MALDI-MSI measurements. MALDI–MSI was performed using single reflectron-type MALDI–time-of-flight (TOF)-MS (AXIMA Confidence, Shimadzu). Quadrupole ion-trap (QIT)-type (AXIMA QIT, Shimadzu) and TOF/TOF type (AXIMA Performance, Shimadzu) instruments were used for identification of metabolites by MS/MS analysis. These instruments were equipped with a 337-nm nitrogen laser and all measurements were performed in both positive and negative ionization reflectron modes with 50 μm spatial resolution (10 laser shots/data point). The signals were collected between *m/z* = 80-890 (negative) or between *m/z* = 1000-1400 (positive). A number of peaks derived from metabolites were calculated by in-house script using Python (http://www.python.org). We first detected the peaks derived from the tomato fruit sample as sample peak, and non-tissue peaks on the glass plate were defined as blank peak. These peaks were exported as centroid format, and then isotope peaks were deleted. Of these peaks, sample peaks with the intensity over five times stronger than that of blank peak within the same *m/z* regions were considered

as the net peaks derived from endogenous metabolites. Metabolites were identified or estimated by comparing MS/MS spectra with standard compounds or databases (MassBank, http://www.massbank.jp; METLIN, http://metlin.scripps.edu). Acquired MSI data were processed with a freely available software Biomap (http://ms-imaging.org/wp/). This software was used for creation of two-dimensional ion-density maps, normalization of peak intensity, adjustment of the color scale, and quantification of the ion intensity. All data was merged between optical and ion images.

3.2.4. Quantitative analysis of metabolites with LC–triple quadrupole (QqQ)–MS

The pericarp (epicarp and mesocarp) and locule fractions (100-200 mg) were homogenized in 80% methanol, including 5 μM 10-camphorsulfonic acid (10-CS) for evaluating the extraction efficiency, on ice using dounce tissue grinders. After centrifugation at 15,000 × *g* for 10 min, the supernatant was collected. These samples were filtered using 0.22 μm PTFE filter (EMD Millipore, Billerica, CA, USA). The filtered samples were

analyzed by high-performance liquid chromatography with triple quadrupole (LC–QqQ)–MS (LC8040, Shimadzu, Kyoto, Japan). The instrument was fitted with a Synagi Hydro-RP column (C18, 100 mm × 2.0 mm i.d., Phenomenex, Torrance, CA, USA), ovened at 40˚C. Mobile phase conditions were as follows: linier gradient analysis with mobile-phase A, 10 mM tributylamine (TBA)/15 mM acetic acid in ultra pure water, and mobile-phase B, methanol. After a 3 min isocratic run at 100% of eluting solvent A, the ratio of eluting solvent B was linearly increased to 40% from 3 to 5 min and to 90% from 5 to 7 min. The composition of 90% of the eluting solvent B was maintained for 5 min. For the MS, the instrument was operating an electrospray ionization source in both positive and negative ionization modes. The ionization parameters were performed under the following conditions: capilary voltage, 4.5 and -3.5kV; the nebulizer gas flow, 1.5 L/min, the CDL temperature, 250˚C and heatblock temperature, 400˚C. Multiple reaction monitoring mode with a dwell time of 2s per channel were used for the targeted analysis of 10 metabolites. Identified metabolites were quantified using authentic standards, and then the data were expressed as the ratios (locule/ epicarp) shown in Fig. 3-5.

3.2.5. Heat map analysis

We used heat map analysis to determine the certainty of the present 9-AA-based MALDI–MSI results by comparing MSI relative peak intensities in both locule and mesocarp regions with LC–MS-quantified data on both locule and pericarp (epicarp and mesocarp) regions in MR tomato fruit. In the MSI experiment, we focused on both locule and mesocarp regions. Regions of interest (ROIs), indicated in Fig. 3-5B, were established in a part of homogenous-tissue regions on the optical image of MR tomato fruit by using BioMap software. Each average intensity from averaged mass spectrum of either locule or mesocarp region determined within selected ROIs. The data was converted into the ratio of locule to mesocarp region. In LC–MS experiments, the epicarp could not be perfectly separated from the mesocarp using fresh fruit. Therefore, we used both mesocarp and pericarp fractions as a crude mesocarp fraction, even though it includes a small amount of epicarp. The metabolite concentration data of LC–MS was converted into the ratio of locule to pericarp region. We compared the ratios between MALDI–MSI and LC–MS using the heat map analysis. The ratio of 10 common metabolites was visualized with MultiExperiment Viewer (http://www.Tm4.org). In this experiment, we used three replicate data for LC–MS analysis and four replicate data for MALDI–MSI analysis. These averaged values were subjected to

the heat map analysis.

3.2.6. Evans Blue staining

Fresh wounding tomato fruit including wound region cut using a razor blade were stained with 0.5% (v/v) Evans Blue solution (Wako Pure Chemical Industries) partially modified from previous report (Kawai M. and Uchimiya H. 2000). After 5 min, the fruit was washed with distilled water and put on the slide glass. This sample was subjected to light microscope (AS-3100, Microadvance, Osaka, Japan). Non-viable cells had blue coloration and viable ones were not stained.

3.3. Results

3.3.1. MALDI–MSI-based visualization of spatial distributions of metabolites in MR tomato fruit

To perform MALDI–MSI experiments, solid samples are thinly sectioned and mounted onto a conductive stage. In this study, we prepared the thin-sections of frozen fruit using a cryomicrotome without any embedding materials, and then the sections were mounted onto indium tin oxide (ITO)-coated glass slides using the thaw-mounting method. The shape of each organ structure, including epicarp, mesocarp, locule and seed, was maintained in the cryosections (Fig. 3-1). The choice of the matrix for MALDI–MSI is an important point for metabolite imaging. Here, we used 9-aminoacridine (9-AA) because it is a superior MALDI matrix for ionizing a broad range of negatively-charged metabolites, such as nucleotides, cofactors, phosphorylated sugars, amino acids, lipids and carboxylic acid (Miura D. *et al*. 2010). The choice of matrix deposition method is also important for achieving successful MSI results with high sensitivity and high spatial resolution. Here, we used a method of sublimation coupled with recrystallization because it was highly reproducible and highly

sensitive, and it eliminated the migration of analyte compounds during matrix deposition (Yang J. and Caprioli R.M. 2011, Bouschen W. *et al*. 2010, Shimma S. *et al*. 2013]. The tissue sections of MR tomato fruit were subjected to the matrix deposition and subsequent MALDI–MSI measurement. In total, 91 peaks derived from endogenous metabolites were detected (Fig. 3-2), and 34 of these peaks had unique distributions in the MR tomato fruit (Fig. 3-3). Both the localization and intensity of the peaks were different among the four tissue compartments MR tomato fruit were subjected to the matrix deposition and subsequent MALDI–MSI measurement. In total, 91 peaks derived from endogenous metabolites were detected (Fig. 3-2), and 34 of these peaks had unique distributions in the MR tomato fruit (Fig. 3-3). Both the localization and intensity of the peaks were different among the four tissue compartments (epicarp, mesocarp, locule and seed). Among these, we successfully identified 10 metabolites, including primary metabolites (sour compounds and umami compounds) and secondary metabolite (caffeate), by comparisons with MS/MS spectra of standard compounds (Fig. 3-4, Table 3-1).

MALDI–MSI provides useful information on the distribution of biomolecules over the two-dimensional analytical regions. However, the signal intensity information does not reflect the 'absolute' amounts but the 'relative' amounts of biomolecules. In some cases, the resultant

images do not reflect the relative amount of an analyte in different regions of the same sample because of the differences in the matrix effects, the ion suppressing or enhancing effect, between different regions (Lou X *et al*. 2009, Duncan M.W. *et al*. 2008). We determined the certainty of the present MSI results by comparing MSI relative peak intensities in both locule and mesocarp regions with LC–MS-quantified data on both locule and pericarp (epicarp and mesocarp) regions in the MR tomato fruit. Although, MSI detected the metabolite distributions in the mesocarp and locule regions, but they were hardly confirmed in the epicarp and seed regions. In this experiment, we focused on the locule and mesocarp regions. Each average intensity of both representative locule and mesocarp regions determined within a selected regions of interest (ROIs) (Fig. 3-5). The data was converted into the ratio of locule to mesocarp region. In LC–MS experiments, the epicarp could not be perfectly separated from the mesocarp using fresh fruit; therefore, we used both locule and pericarp fractions as crude mesocarp fractions, even though it included a small amount of epicarp. The metabolite concentration data was converted into the ratio of locule to pericarp region. We compared the ratios between MALDI–MSI and LC–MS data using the heat map analysis. This analysis showed relatively similar tendencies for most metabolite levels, although the values were different in the MSI and LC-MS data (Fig. 3-5). These results showed, for the first time, that

the present MALDI–MSI technique was able to visualize micro-region-specific distributions, with relatively quantitative values, of multiple metabolites simultaneously in the MR tomato fruit.

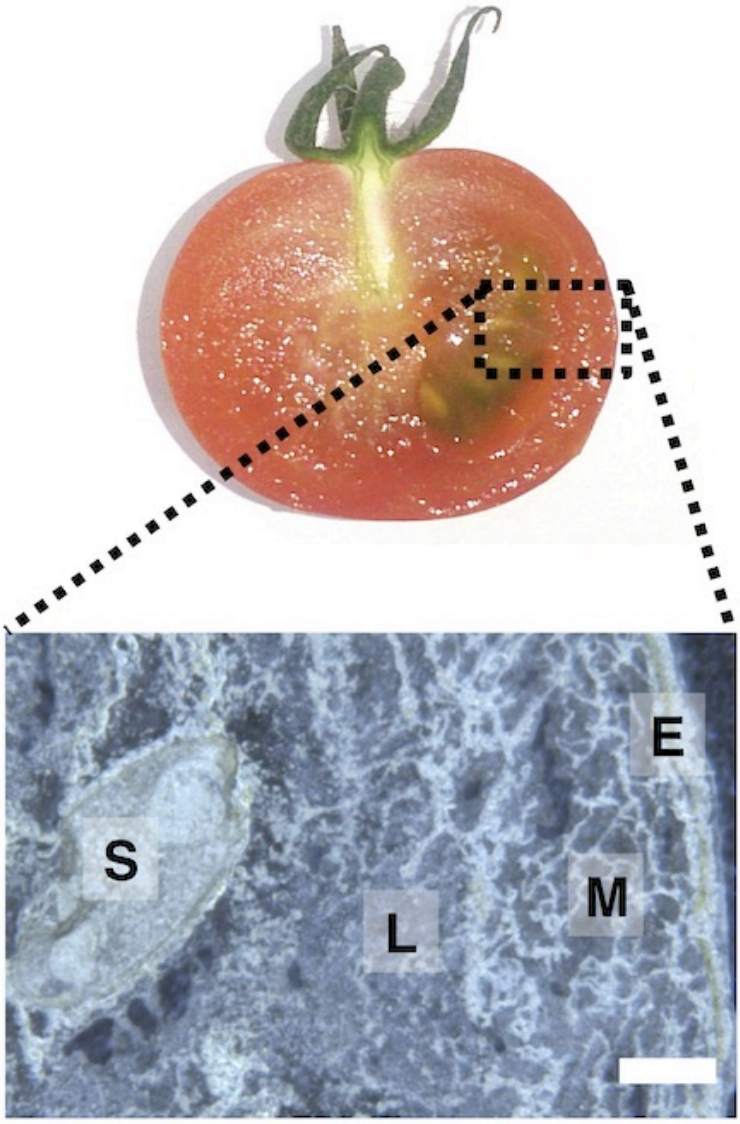

Fig. 3-1 Thin-section of mature red (MR) tomato fruit using cryomictorome without any embedding materials. E ; epicarp, M ; mesocarp, L ; locule, S ; seed. Scale bar = 1.0 mm.

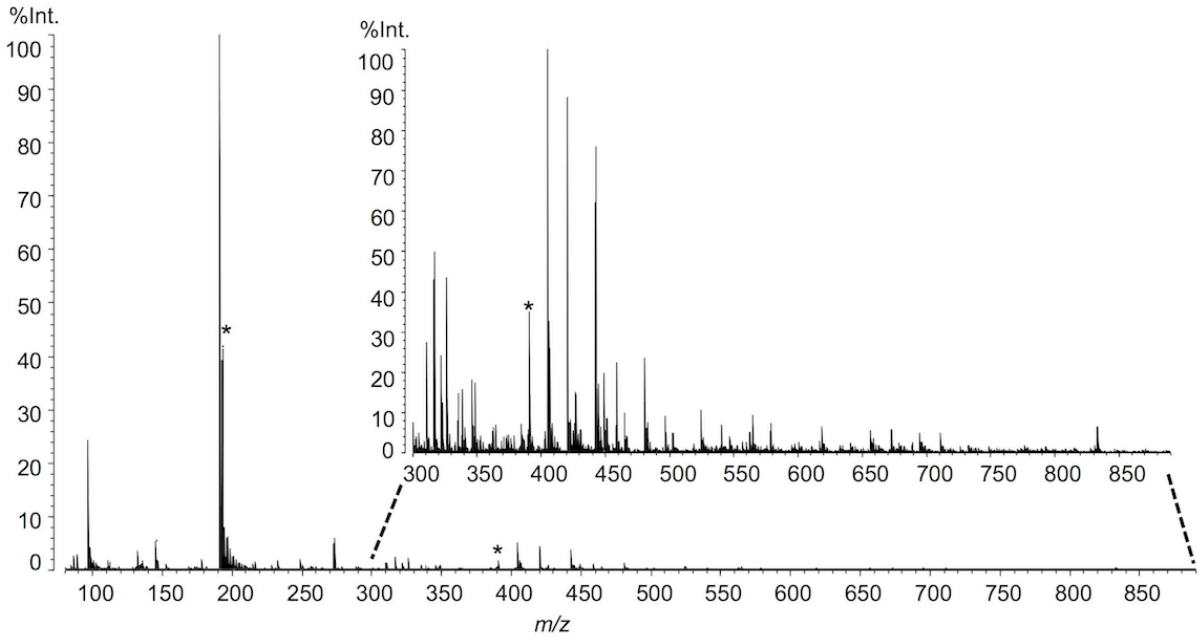

Fig. 3-2 Overview of the averaged mass spectrum acquired from the direct analysis of MR tomato fruit thin section. Whole averaged mass spectrum acquired from MR tomato thin-sections (*m/z* = 80-890). Enlarged spectra from whole averaged mass spectra data (*m/z* = 300-890). Asterisk marks; matrix-derived peaks (matrix: 9-AA).

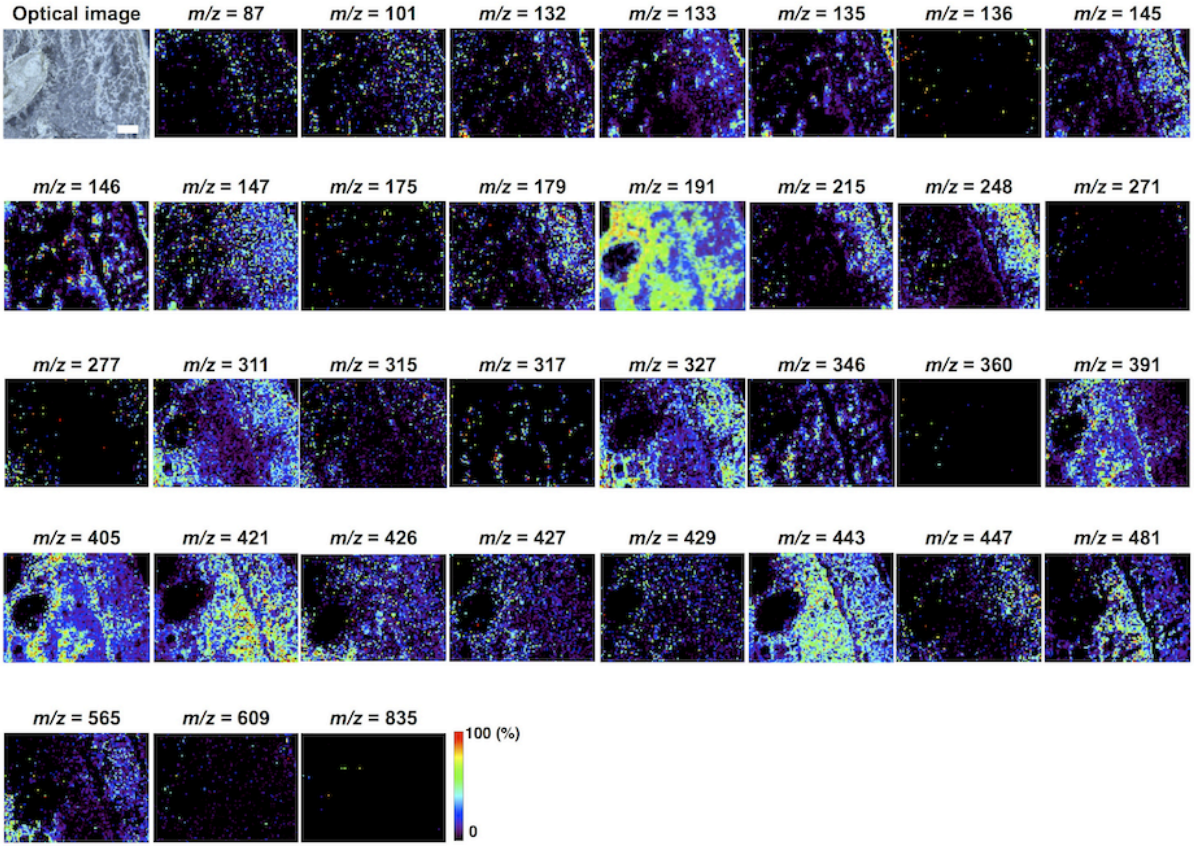

Fig. 3-3 *In situ* compounds imaging of MR tomato fruit section. Visualization of unique distributions of 34 compounds derived from metabolites in the MR tomato fruit section. Scale bar = 1.0 mm.

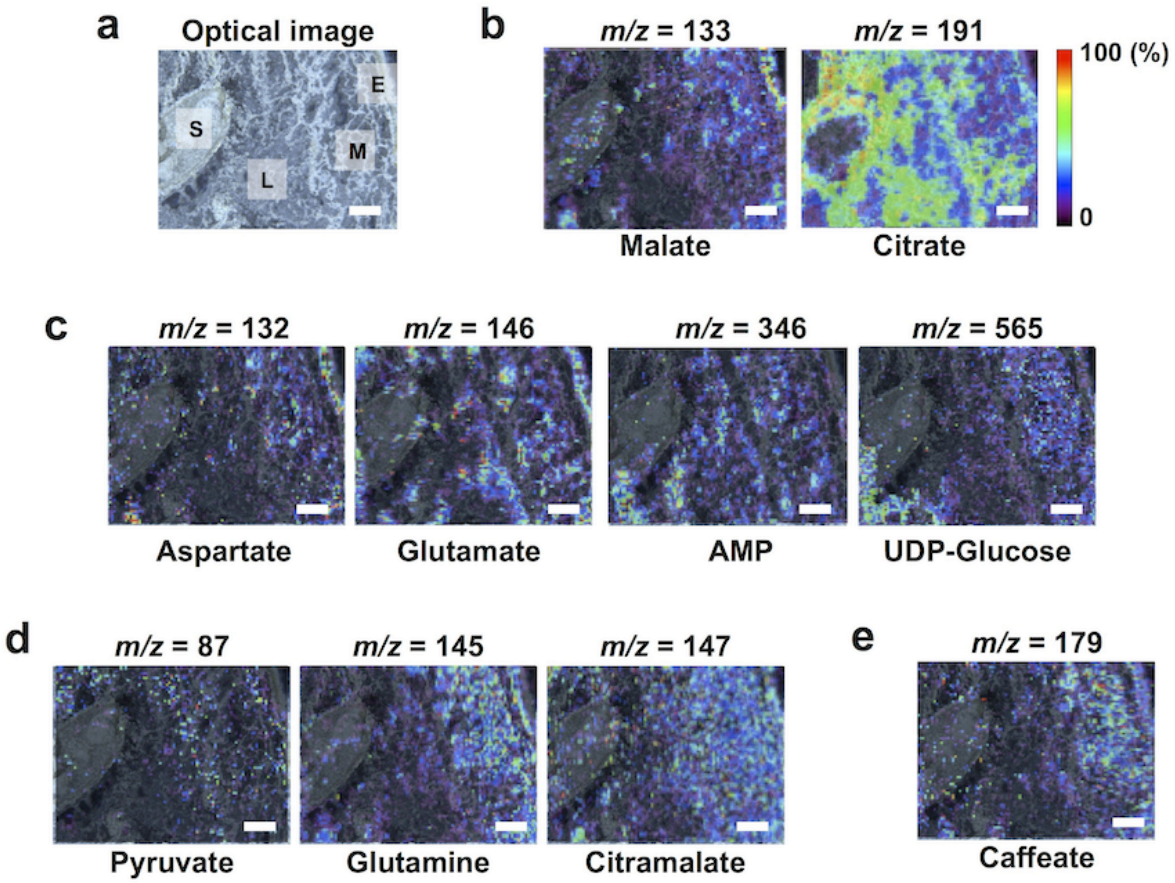

Fig. 3-4 *In situ* metabolite MS imaging of the MR tomato fruit. **a** Optical image of thin-section of the MR tomato fruit. E; epicarp, M; mesocarp, L; locule, S; seed. Ion images of **b** sour compounds, **c** umami compounds, **c** primary metabolites, and **e** secondary metabolite, respectively. Scale bar = 1.0 mm.

Table 3-1 Mass-to-charge ratio, molecular species and fragmentations observed on the tomato fruit section

m/z	*Molecular species*	*Fragments observed*	*Formula*
87	pyruvate	44	$C_3H_4O_3$
132	aspartate	115, 88	$C_4H_7NO_4$
133	malate	115	$C_4H_6O_5$
145	glutamine	127	$C_5H_{10}N_2O_3$
146	glutamate	128, 102	$C_5H_8NO_4$
147	citramalate	129, 101, 87	$C_5H_8O_5$
179	caffeate	135	$C_9H_8O_4$
191	citrate	173, 111	$C_6H_8O_7$
346	AMP	211, 151, 97	$C_{10}H_{14}N_5O_7P$
565	UDP-glucose	403, 323	$C_{15}H_{24}N_2O_{17}P_2$

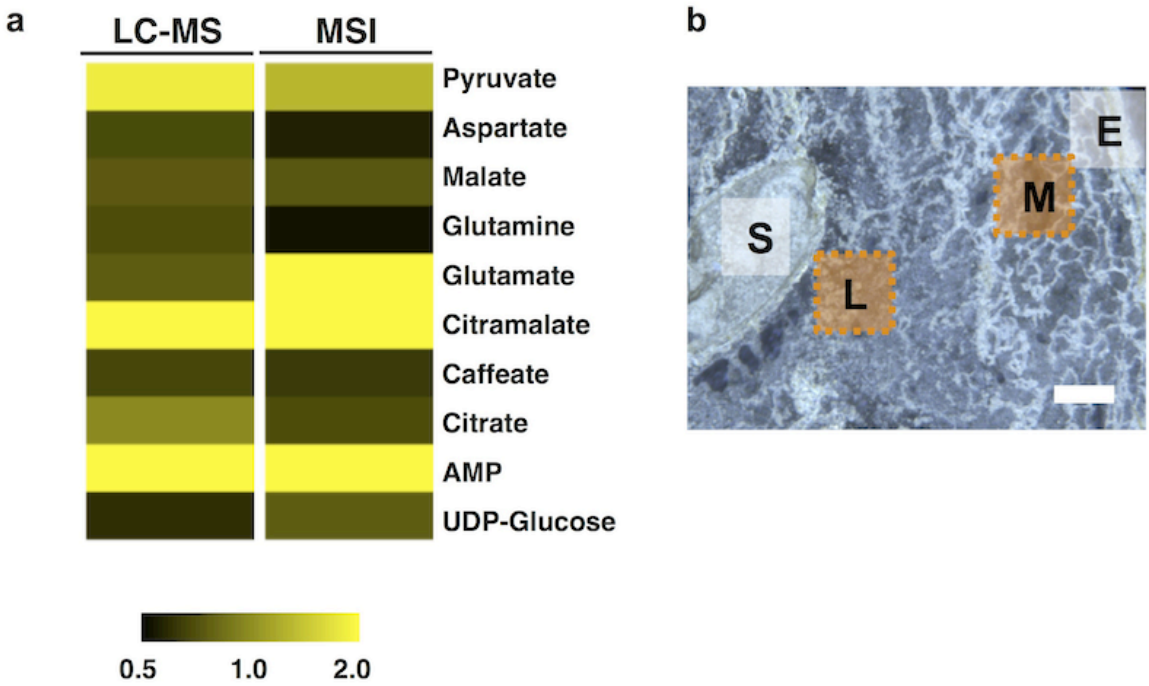

Fig. 3-5 A comparison of the average concentration/intensity between the whole tissue regions and partial tissue regions. **a** In the heat map, 10 common metabolites ratio detected by LC–MS and MSI. The ratio of the average intensity (locule/pericarp) in LC–MS data (left column). The ratio of the average intensity (locule/mesocarp) obtained from ROIs (L) and (M), which are indicated in the panel **b**, in MALDI–MSI data (right column). **b** Optical image of thin-section of the MR tomato fruit. E; epicarp, M; mesocarp, L; locule, S; seed. Scale bar = 1.0 mm.

3.3.2. Analysis of metabolic alterations using two different ripening tomato phenotypes

The concentrations of some taste-related metabolites, such as amino acids and organic acids, change dramatically at the whole-tissue level in tomato fruit during the ripening process (Carrari F. and Fernie A.R. 2006). Additionally, ethylene, a phytohormone, plays a key role in triggering fruit maturation (Alexander L. and Gerierson D. 2002, McAtee P. *et al*. 2013, Osorio S. *et al*. 2013). However, the potential relationships between the presence of metabolites at the tissue micro-regional level and ethylene-induced fruit ripening still remains unclear. Here, we successfully visualized the spatial distribution of multiple metabolites in the MR tomato fruit. To further understand physiological property-related spatiotemporal metabolic alterations, we performed MALDI–MSI experiments using two tomato fruits, MG and MR, of different maturity (Fig. 3-6). The thin-sections of MG and MR were thaw-mounted onto the same conductive glass slide to compare the distributions of multiple metabolites in a single run, and these samples were subject to MALDI–MSI measurement. Metabolite distributions in the mesocarp and locule regions were observed, but they were barely seen in the epicarp and seeds. The amounts of umami compounds, glutamate (*m/z* =

146 [M–H]$^-$) and adenosine monophosphate (AMP) (*m/z* = 346 [M–H]$^-$), were increased in both regions of the MR fruit. Aspartate (*m/z* = 132 [M–H]$^-$), another umami compound, was increased only in a mesocarp region. In contrast, malate (*m/z* = 133 [M–H]$^-$), a constituent of sourness in immature fruit, had decreased compared with in MG fruit. However, the intensities of a secondary metabolite, caffeate (*m/z* = 179 [M–H]$^-$), and other primary metabolite, glutamine (*m/z* = 145 [M–H]$^-$), were similar in the analytical regions of both MG and MR samples (Fig. 3-6). Although there were differences in spatial resolutions, these local metabolic behaviors were in good accordance with the results of whole-tissue extractions from both ripening phenotypes, MG and MR, as previously reported by GC–MS and LC–MS (Oruna-Concha M.J. 2007). Using MALDI–MSI, we succeeded in analyzing the spatiotemporal metabolic alterations in both mesocarp and locule regions during the ripening process of tomato fruit.

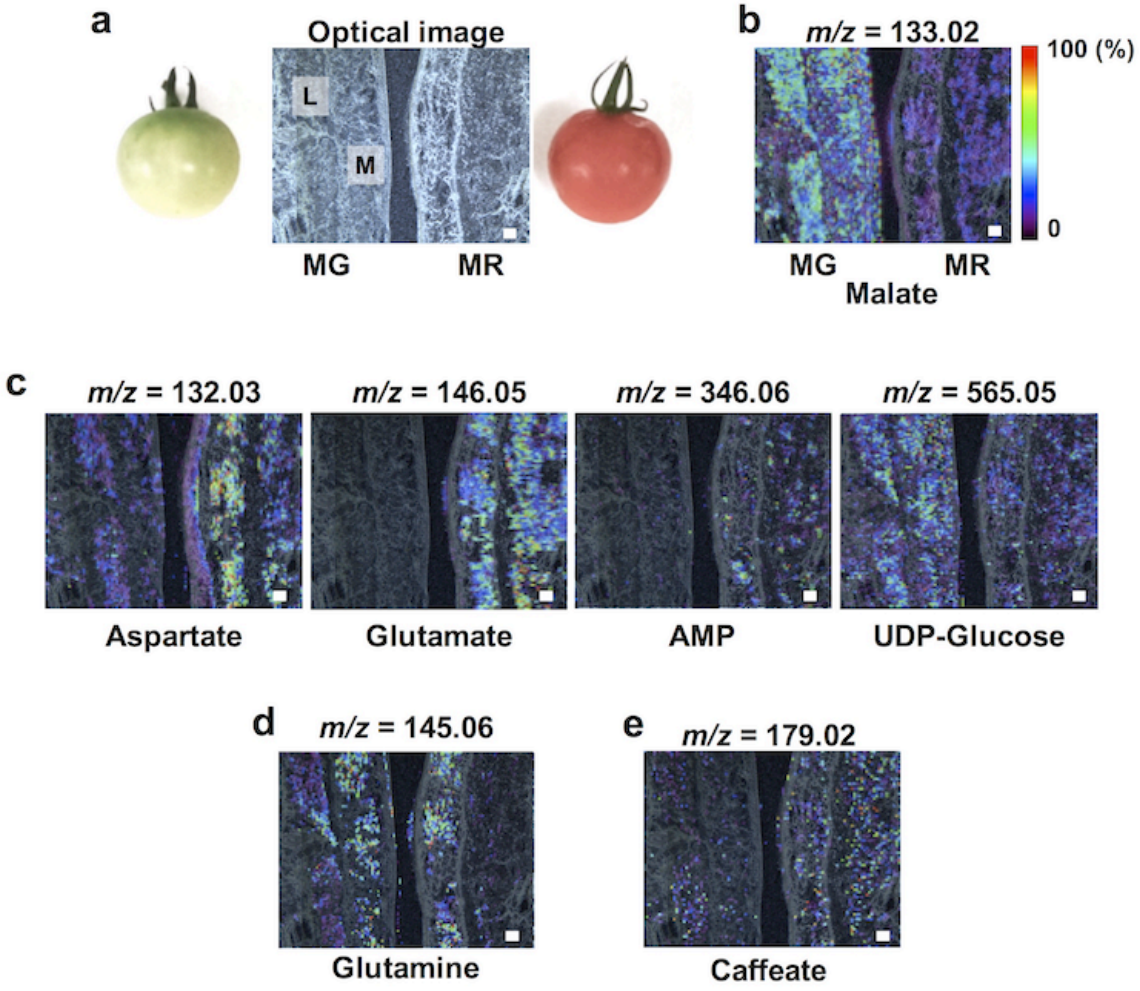

Fig. 3-6 Analysis of the metabolic changes during the progression of ripening process using different ripening phenotypes with 9-AA-based MALDI–MSI. **a** Optical image of thin-sections of the mature green (MG) and MR tomato fruits. M; mesocarp, L; locule. Ion images of **b** sour compound, **c** umami compound, **d** primary metabolites, and **e** secondary metabolite. Scale bar = 1.0 mm.

3.3.3. Spatiotemporal metabolic visualization of local physiological responses to ripening and wounding stress

Plants produce ethylene during wounding stress, and it triggers various genetic and metabolic responses, but the details of these response mechanisms are not fully understood (Saltveit M.E. 2000, Baldassarre V. *et al*. 2015). In particular, local responses near the wound region are still unknown because conventional methods have not been able to assess the cooperative behaviors of multiple biomolecules at the micro-regional level. Here, a 9-AA-based MALDI–MSI analysis was performed to examine metabolic changes around the wound region in the tomato fruit during the ripening process after wounding. We used MG as a control for the beginning stage of ripening and the pink-stage (P) fruit corresponding to the mid-stage, in which less than 60% of the pericarp had changed from green to red during the ripening. The wounded sample (W) was prepared by wounding the MG tomato and at ripening stages up to the P stage. The non-wounded fruit at the corresponding ripening stages were defined as NW. We focused on the locule and mesocarp regions among MG, NW and W fruits. First, we compared the difference between MG and P to determine the metabolic changes that occurred from the beginning to the mid-stage of maturation. In addition, we

determined the differences in the metabolite distributions between NW and W fruits to investigate wound-specific metabolic alterations. As shown Fig. 3-7, an increase in the amount of glutamate and AMP, umami compounds, in P (NW and W) was observed in the local region as compared with MG. However, clear differences between NW and W were not observed among wound-specific metabolic responses to wounding. Next, we used the spray-coating method with 2,5-dihydroxybenzoic acid (DHB) as the matrix to detect other metabolites in the positive ionization mode. DHB-based MALDI–MSI detected tomatine (*m/z* = 1035 $[M+H]^+$), a glycoalkaloid, in MG tissue, and it especially accumulated in both locule and mesocarp regions (Fig. 3-8 a, c). In contrast, the same tomatine distribution was not observed in MR tissue. In addition, there was no accumulation of tomatine at the mid-stage of the ripening process, P (NW) (Fig. 3-8b). Thus, tomatine was lower during the ripening process. In contrast, a putative tomatine-glycosylated metabolite, esculeoside A (*m/z* = 1271 $[M+H]^+$) (Iijima Y. *et al.* 2013), was observed in P, but there was no accumulation in MG (Fig. 3-8 b, c, Fig. 3-9). This tendency was inversely correlated with the presence of tomatine. Additionally, a magnified MSI data showed that, regardless of the mid-stage, tomatine accumulated in the wounded regions of W tissues (Fig. 3-8 d). Esculeoside A showed an inverse presence in the same region. Evans Blue staining revealed cell death around the

wound region, which was the representative physiological response against wounding stress (Fig. 3-8 e). Thus, an alteration in the metabolism of tomatine may be caused by wound-induced cell death. These findings indicate that the MALDI–MSI technique is an effective approach for determining the spatially-resolved metabolism of a glycoalkaloid, tomatine, based on local responses to the ripening process and wounding stress.

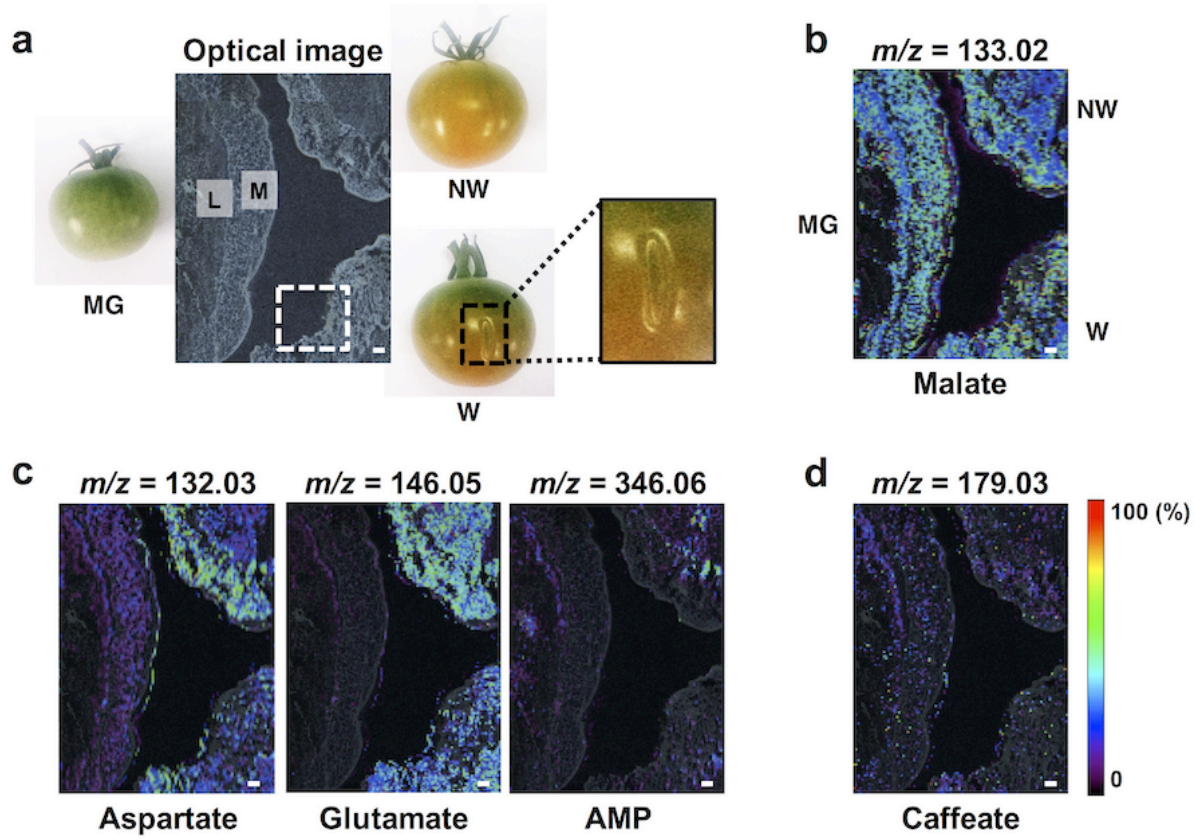

Fig. 3-7 Analysis of metabolic alterations in the wounding stress in the tomato fruit with 9-AA-based MALDI–MSI. **a** Optical image of thin-sections of MG, non-wounded (NW), and wounded (W) tomato fruits. Both NW and W fruits in pink stage, corresponding to the mid-stage of ripening. M; mesocarp, L; locule. The white square indicates the wound region in tomato tissue Ion images of **b** sour compound, **c** umami compounds, and **d** secondary metabolite. Scale bar = 1.0 mm.

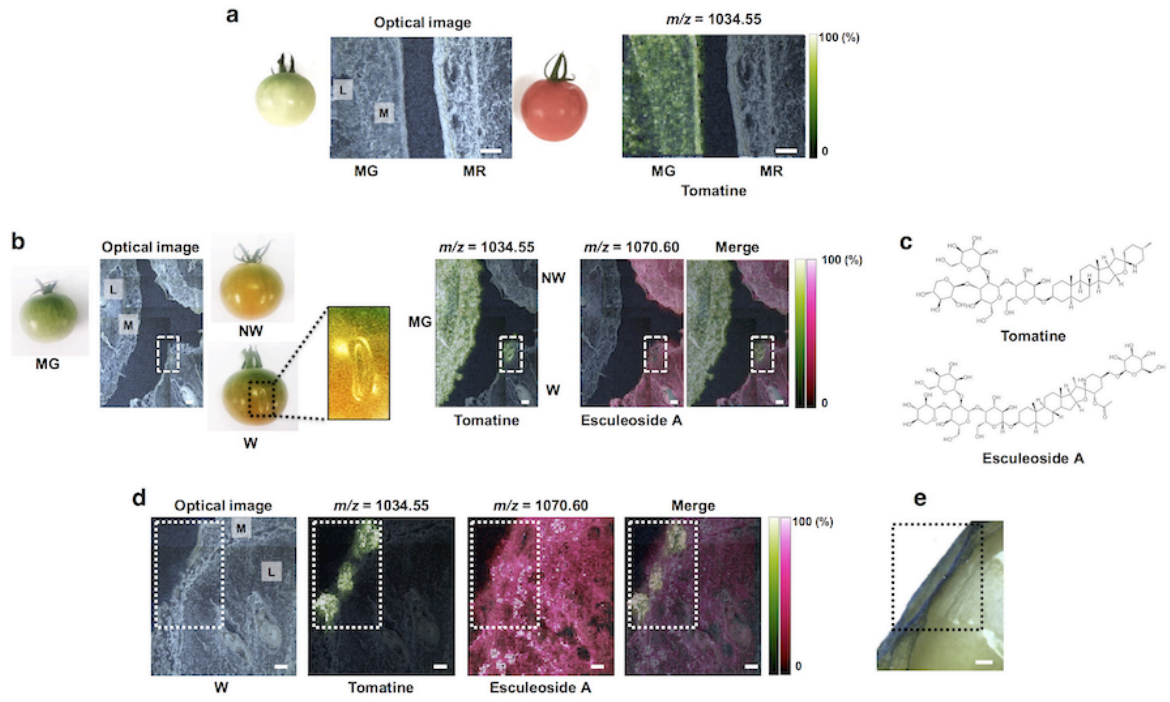

Fig. 3-8 Visualization in more local physiological responses to ripening and wounding stress with DHB-based MALDI–MSI. **a** Optical image and ion image of tomatine in thin-sections of between MG and MR tomato fruits. M; mesocarp, L; locule. **b** Optical image and ion images derived from tomatine-related compounds among three phenotypes of tomato fruits, MG, non-wounded (NW), and wounded (W). Both NW and W fruits in pink stage, corresponding to the mid-stage of ripening. **c** Structures of tomatine (*m/z* = 1035 $[M+H]^+$) and esculeoside A (*m/z* = 1271 $[M+H]^+$), a glycosylated tomatine product. **d** Optical image and magnified ion images derived from tomatine-related compounds focused on the wound region. **e** Evans Blue staining for viability of the cells around wound region in tomato fruit. Blue-colored area; non-viable cells. The broken box; wound region. Scale bar = 1.0 mm.

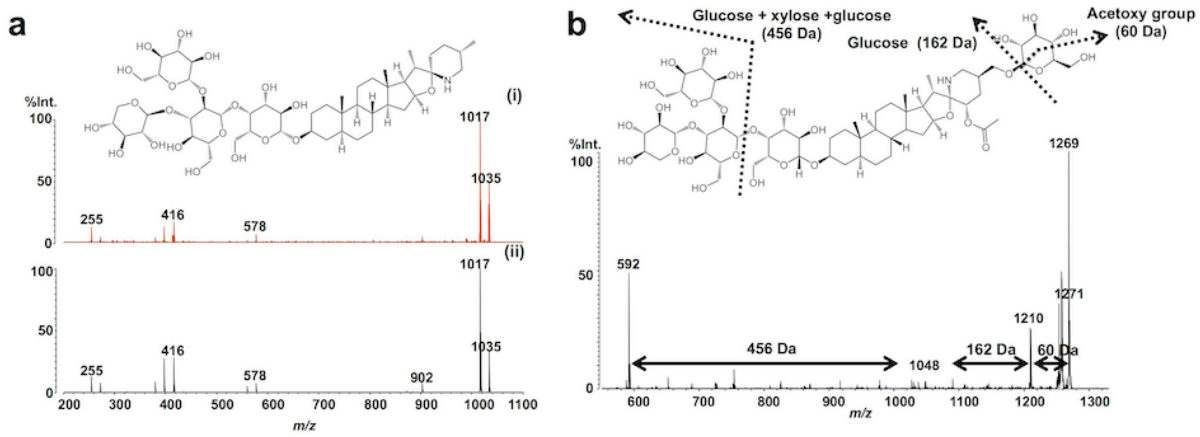

Fig. 3-9 Identification or estimation of compounds derived from glycoalkaloids by comparing with MS/MS data. **a** Identification of MS peaks of *m/z* = 1035 ($[M+H]^+$) as tomatine by comparing with MS/MS spectra between tomato fruit section and standard compound. (i) The MS/MS spectrum acquired from the tomato fruit section. (ii) The MS/MS spectrum of tomatine acquired from standard sample. **b** Estimation of MS peaks of *m/z* = 1271($[M+H]^+$) as esculeoside A by MS/MS data. The fragments were referred from Iijima Y. *et al*. 2013.

3.4. Discussion

In plants, the production of endogenous metabolites is strictly regulated by the complicated signal transduction pathways of the various organs at each growth stage. In particular, there are dynamic changes in the levels of primary and secondary metabolites during developmental processes, such as seed germination, flowering, ripening, and organ abscission (Oikawa A. *et al*. 2015, Tanou G. *et al*. 2015). The climacteric stage of fruit ripening process in tomato and banana (*Musa* spp.) is associated with the increased production of ethylene and a brief increase in cellular respiration (Fig. 3-10). Ethylene is necessary to trigger fruit ripening and senescence processes, but the interaction of ethylene with other signaling pathways is not fully understood (Bouchez O. *et al*. 2007, Fig. 3-11). Thus, elucidating the potential relationships among ethylene-related events and metabolic dynamics during the maturation processes in fruit improves our understanding of the mechanisms responsible for phenotype formation, including color, flavor, taste and morphology. Recently, the MALDI–MSI technique has received increasing attention as an attractive method to determine the spatial distribution of biomolecules in plant materials, such as blueberry, rice grain and Arabidopsis leaves (Yoshimura Y. *et al*. 2012, Zaima N. *et al*.

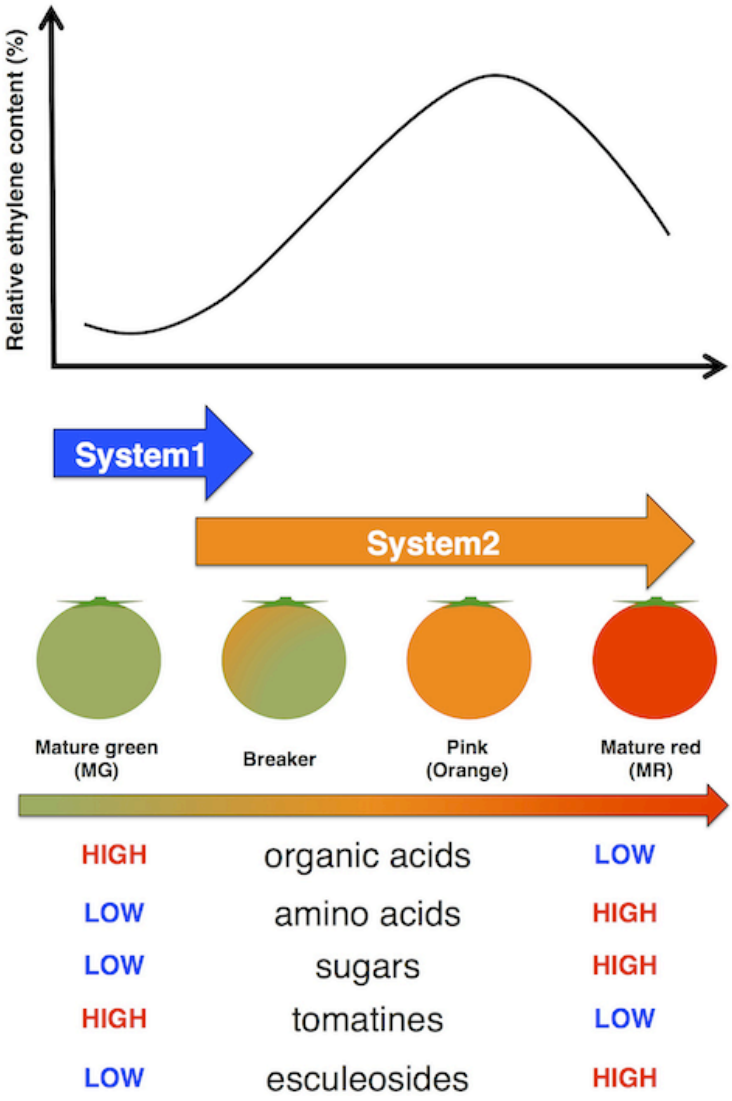

Fig. 3-10 Relationship between ethylene content and dynamics of low-molecular-weight compounds. System1; the autoinhibitory, System2; the autocatalytic. Breker; the color from green to tannish-yellow, pink or red on not more than 10% of the surface.

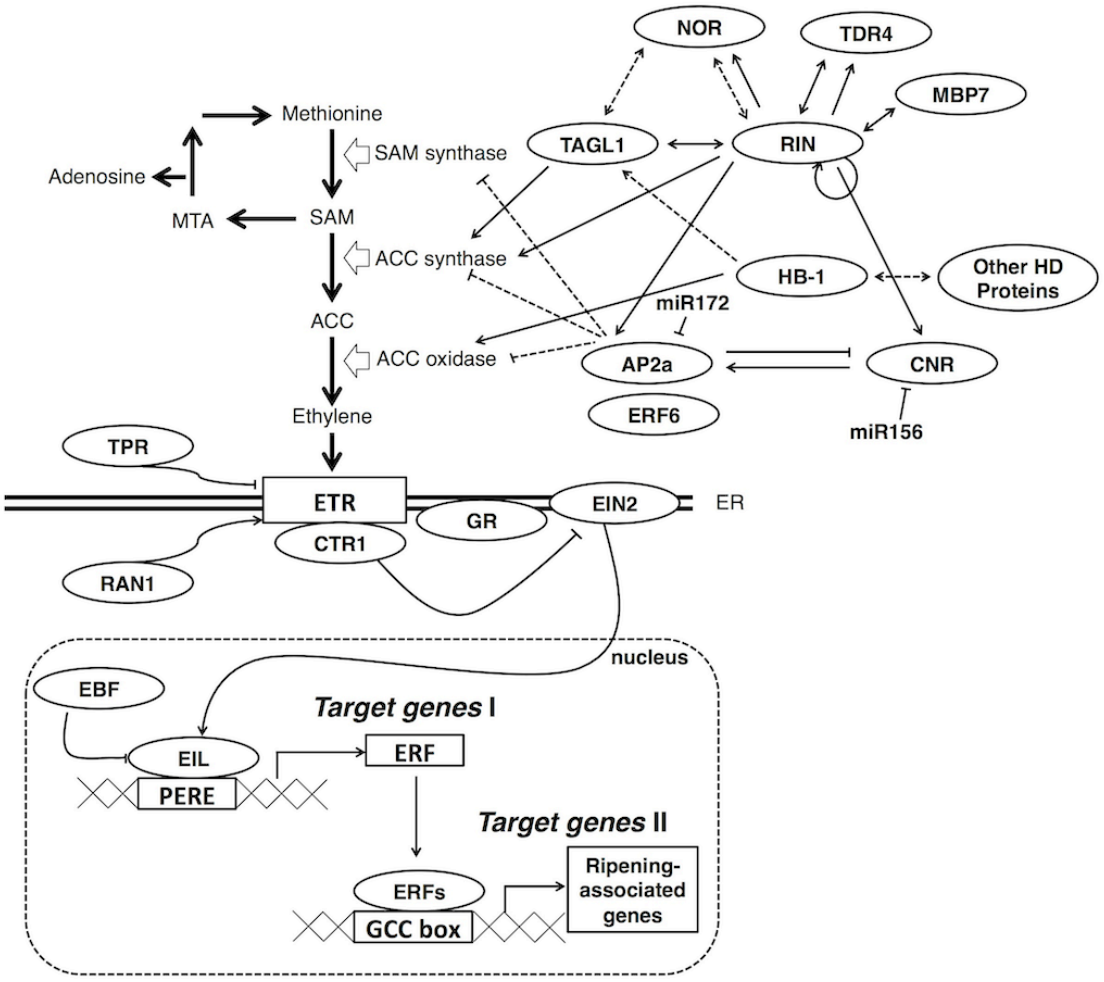

Fig. 3-11 Mechanisms of signal transduction by ethylene. MTA; 5'-methylthioadenosine, SAM; S-adenosylmethionine, ACC; 1-aminocyclopropane-1-carboxylic acid, ETR; ethylene receptor, TPR; tetratricopeptide repeat, RAN; response to antagonist, CTR; constitutive triple response, GR; glucocorticoid receptor, EIN; ethylene-insensitive, EBF; ethylene binding factor, EIL; Ein3-like, PERE; primary ethylene response element, ERF; ethylene responsive factor, NOR; non-ripening, TDR; tapetum degeneration retardation, TAGL; tomato agamous-like, RIN; ripening inhibitor, MBT; tomato fruitfull (FUL2), HB; homoglobin, HD; homeodomain, AP2; apetara 2, CNR; coloress non ripening.

2010, Shroff R. *et al*. 2015). Here, we applied a 9-AA-based MALDI–MSI technique to elucidate the spatial distribution of metabolites in complex tomato fruit structures (epicarp, mesocarp, locule and seed). We were able to visualize, for the first time, the distribution of multiple primary and secondary metabolites simultaneously within tissue sections of MR tomato fruit in a single run. The concentration of an organic acid, malate, at the whole-tissue level gradually increases at the early growth stage, and then it decreases as the ripening process progresses in tomato, while another organic acid, citrate, increases during the late developmental stages (Osorio S. *et al*. 2012). However, little is known about their alterations at tissue micro-regional levels. To reveal metabolite spatiotemporal alterations, including those of the associated organic acids, we performed MALDI–MSI experiments using MG and MR fruits, which were at different stages of maturity. The amount of glutamate and AMP, umami-related compounds, increased in both the mesocarp and locule compartments of the fruit tissue during the ripening progression from MG to MR, while malate, a sour compound, decreased in both regions (Fig. 3-6). Generally, the pericarp's color and taste, such as sour, sweet, and umami, dramatically change during the ripening process. They are related to metabolic alterations, such as the accumulation of carotenoids and amino acids, and ethylene effects, such as the decrease of organic acids (Alexander L. and Gerierson D. 2002, McAtee P.

et al. 2013). When combined with the whole-fruit level findings, our data provide evidence of new relationships between such phenotypes and spatially-resolved metabolic changes during the ethylene-induced progression of ripening in the tomato fruit.

The MALDI–MSI analyzed local metabolic responses against wounding stress and determined the spatial distributions of both tomatine and its glycolated metabolite, esculeoside A, in the tomato fruit (Fig. 3-8). Tomatine is a glycoalkaloid and is involved in host defenses against phytopathogens by inhibiting their activities (Friedman M. 2013). In addition, plants protect themselves by releasing phytoalexin, an antibacterial agent, when they are attacked by pests. Immature green fruit has a high concentration of tomatine in the epicarp region, but its concentration decreases in the MG fruit (Minz-Oron S. *et al*. 2008, Iijima Y. *et al*. 2008). However, the level of tomatine was still unknown in the P stage, which corresponds to the mid-term of the ripening process. In this study, the localization of tomatine was determined in fruit at three different developmental stages (MG, P and MR). In addition, its tomatine-glycolated product, esculeoside A, showed an inverse presence with tomatine between the MG and P. Alterations of tomatine and esculeoside A were present in regions where cell death was induced by wounding. This is the first report demonstrating a spatially-resolved metabolic alteration of a glycoalkaloid based on physiological changes and

responses, such as ripening and wounding, respectively. The existence of genes and proteins concerned with biosynthesis of tomatine in tomato fruit have been reported (Itkin M. *et al*. 2013, Cárdenas P.D. *et al*. 2016), but there were few observations of gene and protein expression levels associated with the glycolation pathway of glycoalkaloid, even though the tomato genome has been sequenced (The tomato genome consortium 2012). Thus, the glycolation mechanism from tomatine to esculeoside A was still unclear. Our findings implicate cell death-related biochemical events in the alterations of tomatine and esculeoside A. A better understanding of this new relationship will shed light on the regulatory mechanisms of glycoalkaloids and their biological significance in local physiological responses against wound-related stress.

In MALDI–MSI, spray-coating method with an airbrush has been used to apply the matrix solution on sample tissues because it is a simple and convenient technique. Thus, DHB-based MALDI–MSI was performed to visualize the distribution of tomatine-derived compounds with high sensitivity using this method (Fig. 3-8 a-c). In particular, this technique determined the spatial distribution of esculeoside A with a higher sensitivity than the sublimation coupled with recrystallization method (data not shown). The spray-coating technique often requires manual operation, and the quality of the resultant sample is completely dependent on the

user's skill. In some cases, this method has shown poor reproducibility (Gemperline E. *et al*. 2014). Here, sublimation and its combination with recrystallization method was used as the matrix deposition strategy. Sublimation was previously reported to be suitable for the detection of glucosinolates in Arabidopsis leaves (Shroff R. *et al*. 2015). The application of the matrix, and the monitoring of its thickness, are performed by fully automated equipment, which is easily operated, leading to a low human error. Furthermore, the sublimation method is suitable for the high spatial resolution imaging when compared with the spray-coating method (Hankin J.A. *et al*. 2007). However, the coverage and sensitivity of detectable metabolites were different in the two methods (Gemperline E. *et al*. 2014). In addition to our attempts, considering these circumstances, researchers must select the matrix deposition method suitable for detecting the metabolites of interest.

Using the method of sublimation coupled with recrystallization to apply 9-AA as a matrix, we detected more than 90 peaks derived from endogenous metabolites in the tomato fruit (Fig. 3-3). In addition, we analyzed 9-AA-deposits in tissue samples by sublimation alone, but the numbers and intensities of the peaks derived from endogenous metabolites were lower than those of sublimation coupled with recrystallization (data not shown). In this study, most of the detected peaks could not be annotated (Fig. 3-4, Table 3-1). The metabolites derived from

sample tissue sections were generally identified and/or estimated by comparing MS/MS spectra with those of standard compounds or public databases. However, it is difficult to theoretically annotate compounds for which standard MS/MS spectra or database information is not available. To overcome this problem, we are now developing a methodology of standard compound-independent determinations of elemental compositions using ultrahigh-resolution MS (Miura D. *et al*. 2010, Nagao T. *et al*. 2014). In addition, optimizing multiple faces of the experimental conditions, including matrix selection, matrix synthesis, and matrix application methods, are required to improve the sensitivity and coverage of detectable metabolites using the MALDI–MSI technique. Improving these factors may help to elucidate the complex mechanisms of physiological changes and responses by visualizing detailed metabolic alterations at tissue micro-regional levels and link them with given phenotypical characteristics.

3.5. Concluding Remarks

Conventional metabolomics approaches are effective approaches for understanding global metabolic alterations in plant tissue. However, these techniques do not address the spatial aspects of more local physiological phenomena, such as metabolic responses against wounding or pest-associated stresses at tissue micro-regional levels. To elucidate the distribution of metabolites in the complex structures of tomato fruit, we were able to visualize, for the first time, the spatial distribution of multiple primary and secondary metabolites simultaneously within tissue sections of MR tomato fruit using 9-AA-based MALDI–MSI combined with the matrix sublimation/recrystallization method. Moreover, we performed a MALDI–MSI experiment using MG and MR fruit, which are at different maturity stages, to further understand the physiological properties related to spatiotemporal metabolic alterations. The amount of umami compounds was high in both locule and mesocarp regions during the ripening process. In contrast, the level of sour compounds was low in both regions. Furthermore, DHB-based MALDI–MSI was applied to evaluate micro-region-specific metabolic alterations in response to wounding stress. We succeeded in visualizing alterations between tomatine and its glycosylated product, esculeoside A, in the wound region. These

new findings suggest that our MSI technique will contribute to an enhanced understanding of physiological alterations of tomato fruits, and may lead to the creation of new plant breeding and postharvest technology.

Chapter 4.

Final remarks on the applications of metabolomic approaches in plants

To obtain better insight into complex biochemical processes, metabolomics data are required not only for the elucidation of the molecular entities involved but also for the determination of their spatial distribution in the organism. The spatial dynamics of metabolites across cells is fundamental to their ability to maintain the viability of the organism. In the present study, the 9-AA-based MALDI-MSI technique enables the simultaneous visualization of the spatial distribution of multiple primary and secondary metabolites within a tissue section of tomato fruit. Additionally, the technique was also used to understand the physiological properties associated with spatiotemporal metabolic alteration during the ripening process. Furthermore, DHB-based MALDI-MSI was applied to assess the micro-region-specific metabolic response to wounding stress. Tomatine and its glucosylated metabolite, esculeoside A, were successfully visualized and specific alterations around the wound region were characterized. This technique will contribute to improving our understanding of the physiological alterations in plant tissues.

In plant science, metabolic pathways and the significance of many secondary metabolites remain unclear. Information on spatiotemporal metabolic dynamics is indispensable for a precise understanding of phenylpropanoids, including the polyphenol, lignin, which is contained in large amounts in plants. Several researchers have attempted to ionize

low-molecular-weight compounds and visualize their spatiotemporal distribution using MALDI-MSI systems (Yoshimura Y. *et al*. 2012, Kim Y.H. *et al*. 2013). However, this work has not improved our detailed understanding of the studied biosynthetic pathways, although the enzymes regulating the pathways are almost completely identified (Vogt T. 2010). Tomatine and esculeoside A are categorized as glycoalkaloids (GAs), natural compounds that exist widely in Solanaceae plants. MALDI-MSI was used to visualize the distribution of the GAs, α-solanine and α-chaconine, in the buds of the potato (*Solanum tuberosum* L.) tuber in a previous study (Ha M. *et al.* 2012). The genes and proteins involved in the biosynthesis of tomatine, α-solanine, and α-chaconine were reported in previous studies (Itkin M. *et al*. 2013, Cárdenas P.D. *et al.* 2016). However, very few studies reported the genes and/or proteins involved in the glycoalkaloid degradation pathway, although the tomato genome had already been sequenced (The Tomato Genome Consortium, 2012). Currently, using conventional metabolome techniques to analyze tomatine and its degradation products from a wild-type plant and two mutants (*rin*; ripening-inhibitor and *nor*; non-ripening), it was shown that they do not exhibit ripening-associated ethylene production (Iijima Y. *et al.* 2008). Conventional metabolome techniques are also expected to further progress GAs research by helping to define the pathway for the biosynthetic decomposition of GAs on the basis of the law of

chemical modification (Schwahn K. *et al.* 2014). Therefore, integrated technologies between conventional metabolome techniques and the present MALDI-MSI method will strongly contribute to understanding how and where plant specific compounds, such as penylpropanoids and glycoalkaloids, are metabolized.

References

Afendi, F.M., Okada, T., Yamazaki, M., Hirai-Morita, A., Nakamura, Y., Nakamura, K., Ikeda, S., Takahashi, H., Alataf-UI-Amin, M., Darusman, L.K., Saito, K., Kanaya, S. (2012), "KNApSAcK family databases: integrated metabolite-plant species databases for multifaceted plant research", *Plant Cell Physiol.* **53** (2), e1(1-12).

Alexander, L., Grierson, D. (2002), "Ethylene biosynthesis and action in tomato: a model for climacteric fruit ripening", *J. Exp. Bot.* 53 (377), 2039-2055.

Baldassarre, V., Cabassi, G., Spadafora, N.D., Aprile, A., Müller, C.T., Rogers, H.J., Ferrante, A. (2015), "Wounding tomato fruit elicits ripening-stage specific changes in gene expression and production of volatile compounds" *J. Exp. Bot.* **66**(5), 1511-1526.

Baldina, S., Picarella, M.E., Troise, A.D., Pucci, A., Ruggieri, V., Ferracane, R., Barone, A., Fogliano, V., Mazzucato, A. (2016), "Metabolite Profiling of Italian Tomato Landraces with Different Fruit Types" *Front. Plant Sci.* **7**: 664.

Barba, I., de Leon, G., Martin, E., Cuevas, A., Aguade, S., Candell-Riera J., Barrabes, J.A., Garcia-Dorado, D. (2008), "Nuclear magnetic resonance-based metabolomics predict sexercise-induced ischemia in patients with suspected coronary artery disease" *Magn. Reson. Med.* **60** (1), 27-32.

Bino, R.J., Hall, R.D., Fiehn, O., Kopka, J., Saito, K., Draper, J., Nikolau, B.J., Mendes, P.,

Roessner-Tunali, U., Beale, M.H., Trethewey, R.N., Lange, B.M., Wurtele, E.S., Sumner, L.W. (2004), "Potential of metabolomics as a functional genomics tool", *Trend Plant Sci.* **9** (9), 418-425.

Bouchez, O., Huard, C., Lorrain, S., Roby, D., Balagué, C. (2007), "Ethylene is one of the key elements for cell death and defence response control in the Arabidopsis lesion mimic mutant *vad1*" *Plant Pysiol.* **145**(2), 465-477.

Boughton, B.A., Thinagaran, D., Sarabia, D., Bacic, A, Roessner, U. (2016), "Mass spectrometry imaging for plant biology: a review", *Phytochem. Rev.* **15**, 445-488.

Bouhifd, M., Hartung, T., Hogberg, H.T., Kleensang, A., Zhao, L. (2013), "Review: toxicometabolomics", *J. Appl. Toxicol.* **33**(12), 1365-1383.

Bremer, C., Weissleder, R. (2001), "In vivo imaging of gene expression: MR and optical technologies", *Acad. Radiol.* **8** (1), 15-23.

Brindle, J.T., Antti, H., Holmes, E., Tranter, G., Nicholson, J.K., Bethell, H.W., Clarke, S., Schofield, P.M., McKilligin, E., Mosedale, D.E., Grainger, D.J. (2002), "Rapid and noninvasive diagnosis of the presence and severity of coronary heart disease using ^{1}H-NMR-based metabonomics", *Nat. Med.* **8** (12), 1439-1444.

Bouschen, W., Schulz, O., Eikel, D., Spengler, B. (2010), "Matrix vapor deposition/

recrystallization and dedicated spray preparation for high-resolution scanning microprobe matrix-assisted laser desorption/ionization imaging mass spectrometry (SMALDI-MS) of tissue and single cells" *Rapid Commun. Mass Spectrom.* **24** (3), 55-364.

Caprioli, R.M., Farmer, T.B., Gile, J. (1997), "Molecular imaging of biological samples: localization of peptides and proteins using MALDI-TOF MS", *Anal. Chem.* **69**(23), 4751-4760.

Cárdenas, P.D., Sonawane, P.D., Pollier, J., Bossche, R.V., Dewangan, V., Weithorn, E., Tal, L., Meir, S., Rogachev, I., Malitsky, S., Giri, A.P., Goossens, A., Burdman, S., Aharoni, A. (2016), "GAME9 regulates the biosynthesis of steroidal alkaloids and upstream isoprenoids in the plant mevalonate pathway", *Nat. Comm.* **7**, 10654.

Carrari, F., Fernie, A.R. (2006), "Metabolic regulation underlying tomato fruit development" *J. Exp. Bot.* **57** (9), 1883-1897.

Denkert, C., Budczies, J., Weichert, W., Wohlgemuth, G., Scholz, M., Kind, T., Niesporek, S., Noske, A., Buckendahl, A., Dietel, M., Fiehn, O. (2008), "Metabolite profiling of human colon carcinoma– deregulation of TCA cycle and amino acid turnover" *Mol. Cancer* **7**, 72.

Dettmer, K., Aronov, P.A., Hammock, B.D. (2007), "Mass spectrometry-based metabolomics", *Mass Spec. Rev.* **26** (1), 51-78.

Dixon, R.A., Strack, D. (2003), "Phytochemistry meets genome analysis, and beyond.....", *Phytochem.* **62** (6),815-816.

Duarte, I., Barros, A., Belton, P.S., Righelato, R., Spraul, M., Humpfer, E., Gil, A.M. (2002), "High-resolution nuclear magnetic resonance spectroscopy and multivariate analysis for the characterization of beer", *J. Agric. Food Chem.* **50**(9), 2475-2481.

Duncan, M.W., Roder, H., Hunsucker, S.W. (2008), "Quantitative matrix-assisted laser desorption/ionization mass spectrometry", *Brief Funct. Genomic Proteomic.* **7** (5), 355-370.

Fiehn, O., Kopka, J., Dörmann, P., Altmann, T., Tretheway, R.N., Willmitzer, L. (2000), "Metabolite profiling for plant functional genomics", *Nat. Biotechnol.* **18** (11), 1157-1161.

Fiehn, O., Kopka, J., Tretheway, R.N., Willmitzer, L. (2000), "Identification of uncommon plant metabolites based on calculation of elemental compositions using gas chromatography and quadrupole mass spectrometry" *Anal. Chem.* **72** (15), 3573-3580.

Fiehn, O. (2002), "Metabolomics- the link between genotypes and phenotypes", *Plant Mol.*

Biol. **48** (1-2), 155-171.

Frickenschmidt, A., Frohlich, H., Bullinger, D., Zell, A., Laufer, S., Gleiter, C.H., Liebich, H., Kammerer, B. (2008), "Metabonomics in cancer diagnosis: mass spectrometry-based profiling of urinary nucleosides from breast cancer patients" *Biomerkers* **13** (4), 435-449.

Friedman, M. (2013), "Anticarcinogenic, cardioprotective, and other health benefits of tomato compounds lycopene, α-tomatine, and tomatidine in pure from and in fresh and processed tomatoes" *J. Agric. Food Chem.* **61** (40), 9534-9550.

Gambhir S.S. (2002), "Molecular imaging of cancer with positron emission tomography", *Nat. Rev. Can.* **2**(9), 683-693.

Gemperline, E., Rawson, S., Li, L. (2014), "Optimization and Comparison of Multiple MALDI Matrix Application Methods for Small Molecule Mass Spectrometric Imaging" *Anal. Chem.* **86**(20), 10030-10035.

Guerquin-Kerm, J.L., Wu, T.D., Quintana, C., Croisy, A. (2005), "Progress in analytical imaging of the cell by dynamic secondary ion mass spectrometry (SIMS microscopy)", *Biochim. Biophys. Acta* **1724** (3), 228-238.

Hankin, J.A., Barkley, R.M., Murphy, R.C. (2007), "Sublimation as a method of matrix application for mass spectrometric imaging" *J. Am. Soc. Mass Spectrom.* **18**(9), 1646-1652.

Ha, M., Kwak, J.H., Kim, Y., Zee, O.P. (2012), "Direct analysis for the distribution of toxic glycoalkaloids in potato tuber tissue using matrix-assisted laser desorption/ionization mass spectrometry imaging", *Food Chem.* **133**(4), 1155-1162.

Hayakawa, E., Fujimura Y., Miura, D. (2016), "MSIdV: a versatile tool to visualize biological indices from mass spectrometry imaging data", *Bioimfomatics* (in press, doi: 10.1093/bioinformatics/btw548)

Hewer, R., Vorster, J., Steffens, F.E. Meyer, D. (2006), "Applying biofluid ^{1}H-NMR-based metabonomic techniques to distinguish between HIV-1 positive/AIDS patients on antiretroviral treatment and HIV-1 negative individuals" *J. Pharm. Biomed. Anal.* **41**(4), 1442-1446.

Heuberger, A.L., Broekling, C.D., Lewis, M.R., Salazar, L., Bousckaert, P., Prenni, J.E. (2012), "Metabolomic profiling of beer reveals effect of tempareture on non-volatile small molecules during short-term strage" *Food Chem.* **135**(3), 1284-1289.

Hölscher, D., Dhakshinamoorthy, S., Alexandrov, T., Becker, M., Bretschneider, T., Buerkert,

A., Crecelius, A.C., Waele, D.D., Elsen, A., Heckel, D.G., Heklau, H., Hertweck, C., Kai, M., Knop, K., Krafft, C., Maddula, R.K., Matthäus, C., Popp, J., Schbeider, B., Schubert, U.S., Sikora, R.A., Svatoš, A., Swennen, R.L. (2014), "Phenalenone-type phytoalexins mediate resistance of banana plant (Musa spp.) to the burrowing nematode Radopholus similis", *Proc. Nat. Aca. Sci.* USA **111** (1), 105-110.

Horn, P.J., Korte, A.R., Neogi, P.B., Love, E., Fuchs, J., Strupat, K., Borisjuk, L., Shulaev, V., Lee, Y.J., Chapman, K.D. (2012), "Spatial mapping of lipids at cellular resolution in embryos of cotton", *Plant Cell* **24** (2), 622-636.

Horn, P.J., Silva, J.E., Anderson, D., Fuchs, J., Borisjuk, L., Nazarenus, T.J., Shulaev, V., Cahoon, E.B., Chapman, K.D. (2013), "Imaging heterogeneity of membrane and storage lipids in transgenic Camelina sativa seeds with altered fatty acid profiles", *Plant J.* **76** (1), 138-150.

Iijima, Y., Fujiwara, Y., Tokita, T., Ikeda, T., Nohara, T., Aoki, K., Shibata, D. (2008), "Involvement of ethylene in the assumulation of esculeoside A during fruit ripening of tomato (*Solanum lycopersicum*) ", *J. Agric. Food Chem.* **57**(8), 3247-3252.

Iijima, Y., Watanabe, B., Sasaki, R., Takenaka, M., Ono, H., Sakurai, N., Umemoto, N., Suzuki, H., Shibata, D., Aoki, K. (2013), "Steroidal glycoalkaloid profiling and structures of glycoalkaloids in wild tomato fruit" *Pytochem.* **95**, 145-157.

Inui, T., Tsuchiya, F., Ishimaru, M., Oka, K., Komura, H. (2013), "Different beers with different hops. relevant compounds for their aroma characteristics", *J. Agric. Food Chem.* **61**(20), 4758-4764.

Itkin, M., Heinig, U., Tzfadia, O., Bhide, A.J., Shinde, B., Cardenas, P.D., Bocobza, S.E., Unger, T., Malitsky, S., Finkers, R., Tikunov, Y., Bovy, A., Chikate, Y., Singh, P., Rogachev, I., Beekwider, J., Giri, A.P., Aharoni, A. (2013), "Biosynthesis of Antinutritional Alkaloids in Solanaceous Crops Is Mediated by Clustered Genes" *Science* **341** (6142), 175-179.

Jorge, T.F., Rodrigues, J.A., Caldana, C., Schmidt, R., van Dongen, J.T., Thomas-Oates, J., Antonio, C. (2014), "Mass spectrometry-based plant metabolomics: metabolite responses to abiotic stress", *Mass specrom. Rev.* **35** (5), 620-649.

Johnson, C.H., Ivanisevic J., Suizdak, G. (2016), "Metabolomics: beyond biomarkers and towards mechanisms", *Nat. Rev. Mol. Cell Biol.* **17** (7), 451-459.

Justesen, U., Knuthen, P., Leth, T. (1998), "Quantitative analysis of flavonoids, flavanones,

and flavanones in fruits, vegitables and bevarages by high-performance liquid chromatography with photo-diode array and mass spectrometric detection", *J. Chromatogr. A* **799** (1-2), 101-110.

Kawai, M., Uchimiya, H. (2000), "Coleoptile Senescence in Rice (*Oryza sativa* L.)." *Ann. Bot.* **86**, 405-414.

Kikuchi, J., Shinozaki, K., Hirayama, T. (2004), "Stable isotope labeling of Arabidopsis thaliana for an NMR-based metabolomics approach", *Plant Cell Physiol.* **45** (8), 1099-1104.

Kim, K., Aronov, P., Zakharkin, S.O., Anderson, D., Perround, B., Thompson, I.M., Weiss, R.H. (2009), "Urine metabolomic analysis for kidney cancer detection and biomarker discovery" *Mol. Cell Proteomics* **8** (3), 558-570.

Kim, Y.H., Fujimura, Y., Hagihara, T., Sasaki, M., Yukihira, D., Nagao, T., Miura, D., Yamaguchi, S., Saito, K., Tanaka, H., Wariishi, H., Yamada, K., Tachibana, H. (2013), "In situ label-free imaging for visualizing the biotransformation of a bioactive polyphenol", *Sci. Rep.* **3**, 2805.

Kind, T., Fiehn, O. (2007), "Seven golden rules for heuristic filtering of molecular formulas obtained by accurate mass spectrometry", *BMC Bioinformatics* **8**,105.

Kind, T., Fiehn, O. (2010), "Advances in structure elucidation of small molecules using mass spectrometry", *Bioanal. Rev.* **2** (1-4), 23-60.

Klapper, M., Ehmke, M., Palgunow, D., Böhme, M., Matthäs, C., Bergner, G., Dietzek, B., Popp, J., Döring, F. (2011), "Fluorescence-based fixative and vital staining of lipid droplets in Caenorhabditis elegans reveal fat stores using microscopy and flow cytometry approaches", *J. Lipid Res.* **52** (6), 1281-1293.

Kovacs, H., Moskau, D., Spraul, M. (2005), "Cryogenically cooled probes– a leap in NMR technology", *Prog. Nucl. Magn. Reson. Spectrosc.* **46** (2), 131-155.

Kusano, M., Redestig, H., Hirai, T., Oikawa, A., Matsuda, F., Fukushima, A., Arita, M., Watanabe, S., Yano, M., Hiwasa-Tanase, K., Ezura, H., Saito, K. (2011), "Covering chemical diversity of genetically-modified tomatoes using metabolomics for objective substantial equivalence assessment.", PLoS ONE **6**: e16989.

Last, R.L., Jones D., Shachar-Hill, Y. (2007), "Towards the plant metabolome and beyond", *Nat. Rev. Mol. Cell Biol.* **8** (2), 167-174.

Lee, Y.J., Perdian, D.C., Song, Z., Yeung, E.S., Nikolau, B.J. (2012), "Use of mass spectrometry for imaging metabolites in plants", *Plant J.* **70** (1), 81-95.

Lei, Z., Huhman, D.V., Sumner, L.W. (2011), "Mass spectrometry strategies in metabolomics",

J. Bio. Chem. **286** (29), 25435-25442.

Li, B., Knudsen, C., Hansen, N.K., Jøergensen, K., Kannangara, R., Bak, S, Takos, A., Rook, F., Hansen, S.H., Møller, B.L., Janfelt, C., Bjarnholt, N. (2013), "Visualizing metabolite distribution and enzymatic conversion in plant tissues by desorption electrospray ionization mass spectrometry imaging", *Plant J.* **74** (6), 1059-1071.

Liu, X., Gao, J., Chen, J., Wang Z., Shi, Q., Man, H., Guo, S., Wang, Y., Li, Z., Wang, W. (2016), "Identification of metabolic biomarkers in patients with type 2 diabetic coronary heart diseases based on metabolomic approach", *Sci. Rep.* **6**, 30785.

Lou, X., van Dongen, J.L.J., Vekemans, J.A.J.M., Meijer, E.W. (2009), "Matrix suppression and anlalyte suppression effects of quaternary ammonium salts in matrix-assisted laser desorption/ionization time-of-flight mass spectrometry: an investigation of suppression mechanism.", *Rapid Commun. Mass Spectrom.* **23**(19), 3077-3082.

Maezola, P., Osuculati, F., Sbarbati, A. (2003), "High field MRI in preclinical reserch", *Europ. J. Radiol.* **48** (2), 165-170.

Mashego, M.R., Rumbold, K., Mey, M.D., Vandamme, E., Soetacrt,W., Heijnen, J.J. (2007), "Microbial metabolomics: past, present and future methodologies", *Biotechnol. Lett.* **29**(1), 1-16.

Matsuda, F., Yokota-Hirai, M., Sasaki, E., Akiyama, K., Yonekura-Sakakibara, K., Provart, N.J., Sakurai, T., Shimada, Y., Saito, K. (2010), "AtMetExpress development: a phytochemical atlas of Arabidopsis development", *Plant Physiol.* **152** (2), 566-578.

Matsuda, F., Yonekura-Sakakibara, K., Niida, R., Kuromori, T. Saito, K. (2009), "MS/MS spectral tag-based annotation of non-targeted profile of plant secondary metabolites", *Plant J.* **57** (3), 555-577.

McAtee, P., Karim, S., Schaffer, R., David, K. (2013), "A dynamic interplay between phytohormones is required for fruit development, maturation, and ripening." *Front. Plant Sci.* **4**: 76.

Mintz-Oron, S., Mandel, T., Rogachev, I., Feldberg, L., Lotan, O., Yativ, M., Wang, Z., Jetter, R., Venger, I., Adato, A., Aharoni, A. (2008), "Gene expression and metabolism in tomato fruit surface tissues." *Plant Physiol.* **147**(2), 823-851.

Miura, D., Fujimura, Y., Yamato, M., Hyodo, F., Utsumi, H., Tachibana, H., Wariishi, H. (2010), "Ultrahighly sensitive in situ metabolomic imaging for visualizing spatiotemporal metabolic behaviors.", *Anal. Chem.* **82**(23), 9789-9796.

Miura, D., Fujimura, Y., Wariishi, H. (2012), "In situ metabolomic mass spectrometry imaging: recent advances and difficulties", *J. Proteom.* **75** (16), 5052-5060.

Miura, D., Tsuji, Y., Takahashi, K., Wariishi, H., Saito, K. (2010), "A strategy for the determination of the elemental composition by fourier transform ion cyclotron resonance mass spectrometry based on isotopic peak ratios." *Anal. Chem.* **83**(13), 5887-5891

Nagao, T., Yukihira, D., Fujimura, Y., Saito, K., Takahashi, K., Miura, D., Wariishi, H. (2014), "Power of isotopic fine structure for unambiguous determination of metabolite elemental compositions: in silico evaluation and metabolomic application." *Anal. Chim. Acta.* **27**, 813-816.

Nakamura, J., Morikawa-Ichinose, T., Fujimura, Y., Hayakawa, E., Takahashi, K., Ishii, T., Miura, D., Wariishi, H. (2016), "Spatially resolved metabolic distribution for unraveling the physiological change and responses in tomato fruit using matrix-assisted laser desorption/ionization–mass spectrometry imaging (MALDI–MSI)", *Anal. Bioanal. Chem.* (in press, DOI 10.1007/200216-016-0118-4)

Nielsen, J. (2001), "Metabolic engineering", *App. Microbiol. Biotechnol.* **55** (3), 263-283.

Nordström, A., Lewensohn, R. (2010), "Metabolomics: moving to the clinic", *J. Neuroimmune. Pharmacol.* **5**(1), 4-17.

Oliver, S.G., Winson, M.K., Kell, D.B., Banganz, F. (1998), "Systematic functional analysis of the yeast genome", *Trends Biotechnol.* **16** (9), 373-378.

Oikawa, A., Otsuka, T., Nakabayashi, R., Jikumaru, Y., Isuzukawa, K., Murayama, H., Saito, K., Shiratake, K. (2015), "Metabolic Profiling of developing pear fruits reveals dynamic variation in primary and secondary metabolites, including plant hormones." PLoS ONE **10**, 1371.

Okazaki, Y., Saito, K. (2012), "Recent advances of metabolomics in plant biotechnology", *Plant Biotechnol. Rep.* **6** (1), 1-15.

Osorio, S., Alba, R., Damasceno, C.M.B., Lopez-Casado, G., Lohse, M., Zanor, M.I., Tohge, T., Usadel, B., Rose, J.K.C, Fei, Z., Giovannoni, J.J., Fernie, A.R. (2011), "Systems Biology of Tomato Fruit Development: Combined Transcript, Protein, and Metabolite Analysis of Tomato Transcription Factor (nor, rin) and Ethylene Receptor (Nr) Mutants Reveals Novel Regulatory Interactions", *Plant Physiol.* **157** (1), 405-425.

Osorio, S., Alba, R., Nikoloski, Z., Kochevenko, A., Fernie, A.R., Giovannoni, J.J. (2012), "Integrative comparative analyses of transcript and metabolite profiles from pepper and tomato ripening and development stages uncovers species-secific patterns of network regulatory behavior." *Plant Physiol.* **159**(4), 1713-1729.

Osorio, S., Scossa, F., Fernie, A.R. (2013), "Molecular regulation of fruit ripening.", *Front. Plant Sci.* **4**, 198.

Oruna-Concha, M.J., Methven, L., Blumenthal, H., Young, C., Mottram, D.S. (2007), "Differences in glutamic acid and 5‘-ribonucleotide contents between flesh and pulp of tomatoes and the relationship with umami taste.", *J. Agric. Food Chem.* **55** (14), 5776-5780.

Pope, G.A., MacKenzie, D.A., Defermez, M., Aroso M.A.M.M., Fuller, L.J., Mellon,F.A., Bunn, W.B., Brown, M., Goodacre, R., Kell, D.B., Marvin M.E., Louis, E.J., Roberts, I.N. (2007), "Metabolic footprinting as a tool for discriminating between brewing yeasts", *Yeast* **24**(8), 667-679.

Pace, N.R. (2001), "The universal nature of biochemistry", *Proc. Natl. Acad. Sci. USA* **98** (3), 805-808.

Patti, G.J., Yanes, O., Suizdak, G. (2012), "Metabolomics: the apogee of the omics trilogy", *Nat. Rev. Mol. Cell Biol.* **13** (4), 263-269.

Pyke, J.S., Callahan, D.L., Kanojia, K., Bowne, J., Sahani, S., Tull, D., Bacic, A., McConville, M.J., Roessner, U. (2015), "A tandem liquid chromatography-mass spectrometry (LC–MS) method for profiling small molecules in complex samples", *Metabolomics* **11** (6), 1552-1562.

Roessner, U., Luedemann, A., Brust, L., Fiehn, O., Linke, T., Willmitzer, L., Fernie, A.R.

(2001), "Metabolic profiling allows comprehensive phenotyping of genetically or environmentally modified plant systems", *Plant Cell* **13** (1) 11-29.

Roessner, U., Wagner, C., Kopka, J., Tretheway, R.N., Willmitzer, L. (2000), "Simultaneous analysis of metabolites in potato tuber by gas chromatography–mass spectrometry", *Plant J.* **23** (1), 131-142.

Ruttkies, C., Schymanski, E.L., Wolf, S., Hollender, J., Neumann, S. (2016), "MetFrag relaunched: incorporating strategies beyond in silico fragmentation", *J. Cheminform.* **8**,3.

Saltveit, M.E. (2000), "Wound induced changes in phenolic metabolism and tissue browning are altered by heat shock", *Postharv. Biol. Biotechnol.* **21**(1), 61-69.

Schwahn, K., Perez de Souza, L., Fernie, A.R., Tohge, T. (2014), "Metabolomics-assisted refinement of the pathways of steroidal glycoalkaloid biosynthesis in the tomato clade" *J. Interg. Plant Bio.* **56** (9), 864-875.

Seyer, A., Einhorn, J., Brunelle, A., Laprévote, O. (2010), "Localization of flavonoids in seeds by cluster time-of-flight secondary ion mass spectrometry imaging", *Anal. Chem.* **82** (6), 2326-2333.

Schauer N., Fernie A.R. (2006), "Plant mtabolomics: towards biological function and mechanism", *Trends in Plant Sci.* **11** (10), 508-516.

Shimma, S., Takashima, Y., Hashimoto, J., Yonemori, K., Tamura, K., Hamada, A. (2013), "Alternative two-step matrix application method for imaging mass spectrometry to avoid tissue shrinkage and improve ionization efficiency.", *J. Mass Spectrom.* **48**(12), 1285-1290.

Shroff, R., Schramm, K., Jeschke, V., Nemes, P., Vertes, A., Gershenzon, J., Svatoš, A. (2015), "Quantification of plant surface metabolites by matrix-assisted laser desorption-ionization mass spectrometry imaging: glucosinolates on Arabidopsis thaliana leaves." *Plant J.* **81**(6), 961-972.

Smith, E., Morowitz, H.J. (2004), "Universality in intermediary metabolism", *Proc. Natl. Acad. Sci. USA* **101** (36), 13168-13173.

Soga, T., Ueno, Y., Naraoka, H., Ohashi, Y., Tomita, T., Nishioka, T. (2002), "Simultaneous determination of anioic intermediates for Bacillus subtilis metabolic pathways by capillary electrophoresis electrospray ionization mass spectrometry", *Anal Chem.* **74** (10), 2233-2239.

Soga, T., Ohashi, Y., Ueno, Y., Naraoka, H., Tomita, M., Nishioka, T. (2003), "Quantitative metabolome analysis using capillary electrophoresis mass spectrometry", *J. Proteome Res.* **2** (5), 488-494.

Spevacek, A.R., Benson, K.H., Bamforth, C.W., Slupsky, C.M. (2016), "Beer metabolomics: molecular details of the brewing process and the differential effects of late and dry hopping on yeast purine metabolism", *J. Inst. Brew.* **122**(1), 21-28.

Stoeckli, M., Chaurand, P., Hallahan, D.E., Caprioli, R.M. (2001), "Imaging mass spectrometry: a new technology for the analysis of protein expression in mammalian tissues." *Nature Med.* **7**(4), 493-496.

Takáts, Z., Wiseman, J.M., Gologan, B., Cook, R.G. (2004), "Mass spectrometry sampling under ambient conditions with desorption electrospray ionization", *Science* **36** (5695), 471-473.

Tanou, G., Minas, I.S., Karagiannis, E., Tsikou, D., Audebert, S., Papadopoulou, K.K., Molassiotis, A. (2015), "The impact of sodium nitroprusside and ozone in kiwifruit ripening physiology: a combined gene and protein expression profiling aproach." *Ann. Bot.* **116** (4), 649-662.

Thanbichler, M., Wang, S.C., Shapiro L. (2005), "The bacterial nucleoid: a highly organized and dynamic structure", *J. Cell. Biochem.* **96** (3), 506-521.

The tomato genome consortium. (2012), "The tomato genome sequence provides insights into fleshy fruit evolution.", *Nature* **485** (7400), 635-641.

Thunig, J., Hansen, S.H., Janfelt, C. (2011), "Analysis of secondary plant metabolites by indirect desorption electrospray ionization imaging mass spectrometry", *Anal. Chem.* **83** (9), 3256-3259.

Tohge, T., Fernie, A.R. (2015), "Metabolomics-inspired insight into developmental, environmental and genetic aspects of tomato fruit chemical composition and quality", *Plant Cell Physiol.* **56** (9), 1681-1696.

Tohge, T., Nishiyama, Y. Yokota-Hirai, M., Yano, M., Nakajima, J., Awazuhara, M., Inoue, E., Takahashi, H., Goodenowe, D.B., Kitayama, M., Noji, M., Yamazaki, M., Saito, K. (2005), "Functional genomics by integrated analysis of metabolome and transcriptome of Arabidopsis plants over-expressing an MYB transcription factor", *Plant J.* **42** (2), 218-235.

Tolstikov, V.V., Fiehn, O. (2002), "Analysis of highly polar compounds of plant origin: combination of hydrophilic interaction chromatography and electrospray ion trap mass spectrometry", *Anal. Biochem.* **301** (2), 298-307.

Toubiana, D., Semel, Y., Tohge, T., Beleggia, R., Cattivelli, L., Rosental, L., Nikoloski, Z., Zamir, D., Fernie, A.R., Fait, A. (2012), "Metabolic profiling of a mapping population exposes new insights in the regulation of seed metabolism and seed, fruit, and plant

relations", PLoS Genet. **8** (3), e1002612.

Underwood, B.R., Broadhurst, D., Dunn, W.B., Ellis D.I., Michell, A.W., Vacher, C., Mosedale, D.E., Kell, D.B., Barker, R.A., Grainger, D.J., Rubinsztein, D.C. (2006), "Huntington disease patients and transgenic mice have similar pro-catabolic serum metabolite profiles", *Brain* **129** (Pt4), 877-886.

Yang, J., Caprioli, R.M. (2011), "Matrix Sublimation/Recrystallization for Imaging Proteins by Mass Spectrometry at High Spatial Resolution." *Anal. Chem.* 83 (14), 5728-5734.

Yoshimura Y, Enomoto H, Moriyama T, Kawamura Y, Setou M, Zaima N. (2012), "Visualization of anthocyanin species in rabbiteye blueberry vaccinium ashei by matrix-assisted laser desorption/ionization imaging mass spectrometry." *Anal. Bioanal. Chem.* **403**(7), 1885-1895.

Yukihira, D., Miura, D., Saito, K., Takahashi, K., Wariishi, H. (2010), "MALDI–MS-based high-throughput metabolite analysis for intracellular metabolic dynamics", *Anal. Chem.* **82** (10), 4278-4282.

Vogt, T. (2010), "Phenylpropanoid biosynthesis", *Mol. Plant* **3** (1), 2-20.

Wikoff, W.R., Gangoiti, J.A., Barshop, B.A., Siuzdak, G. (2007), "Metabolomics identifies perturbations in human disorders of propionate metabolism" *Clin. Chem.* **53** (12),

2169-2176.

Wiseman, J.M., Ifa, D.R., Song, Q., Cooks R.G. (2006), "Tissue imaging at atmospheric pressure using desorption electrospray ionization (DESI) mass spectrometry", *Angew. Chem. Int. Ed. Engl.* **45** (43), 7188-7192.

Wishart, D.S. (2008), "Quantitative metabolomics using NMR", *TrAC- Trends Analyt. Chem.* **27** (3), 228-237.

Zaima, N., Goto-Inoue, N., Hayasaka, T., Setou, M. (2010), "Application of imaging mass spectrometry for the analysis of Oryza sativa rice." *Rapid Commun. Mass Spectrom.* **24**(18), 2723-2729.

Zanor, M.I., Rambla, J.L., Chaïb, J., Steppa, A., Medina, A., Granell, A., Fenie, A.R., Causse, M. (2009), "Metabolic characterization of loci affecting sensory attributes in tomato allows an assessment of the influence of the levels of primary metabolites and volatile organic contents" *J. Exp. Bot.* **60** (7) 2139-2154.

Vita

Vita

Junya Nakamura was born in Nagasaki, Japan on February 7, 1986. He received her Bachelor of Agriculture degree from Tokyo University of agriculture, Japan in March, 2010. He immediately continued his study in master degree and received his Master of Science degree from Kyushu University in March, 2012.

In April, 2013, the author joined the PhD program at Graduate School of Bioresource and Bioenvironmental Science, Kyushu University.